AFRL-HE-WP-TR-2000-0156

UNITED STATES AIR FORCE
RESEARCH LABORATORY

Subsonic Aircraft Noise At and Beneath the Ocean Surface: Estimation of Risk for Effects on Marine Mammals

Anthony I. Eller
Raymond C. Cavanagh

SCIENCE APPLICATIONS INTERNATIONAL CORP.
1710 Goodridge Drive
McLean VA 22102

June 2000

Interim Report for the Period October 1996 to April 2000

20011016 166

Human Effectiveness Directorate
Crew System Interface Division
2610 Seventh Street
Wright-Patterson AFB OH 45433-7901

NOTICES

When US Government drawings, specifications, or other data are used for any purpose other than a definitely related Government procurement operation, the Government thereby incurs no responsibility nor any obligation whatsoever, and the fact that the Government may have formulated, furnished, or in any way supplied the said drawings, specifications, or other data, is not to be regarded by implication or otherwise, as in any manner licensing the holder or any other person or corporation, or conveying any rights or permission to manufacture, use, or sell any patented invention that may in any way be related thereto.

Please do not request copies of this report from the Air Force Research Laboratory. Additional copies may be purchased from:

> National Technical Information Service
> 5285 Port Royal Road
> Springfield, Virginia 22161

Federal Government agencies and their contractors registered with the Defense Technical Information Center should direct requests for copies of this report to:

> Defense Technical Information Center
> 8725 John J. Kingman Road, Suite 0944
> Ft. Belvoir, Virginia 22060-6218

TECHNICAL REVIEW AND APPROVAL

AFRL-HE-WP-TR-2000-0156

This report has been reviewed by the Office of Public Affairs (PA) and is releasable to the National Technical Information Service (NTIS). At NTIS, it will be available to the general public.

This technical report has been reviewed and is approved for publication.

FOR THE COMMANDER

MARIS M. VIKMANIS
Chief, Crew System Interface Division
Air Force Research Laboratory

REPORT DOCUMENTATION PAGE			Form Approved OMB No. 0704-0188

1. AGENCY USE ONLY *(Leave blank)*	2. REPORT DATE	3. REPORT TYPE AND DATES COVERED
	June 2000	Interim - Oct 96 to Apr 00

4. TITLE AND SUBTITLE
Subsonic Aircraft Noise At and Beneath the Ocean Surface: Estimation of Risk for Effects on Marine Mammals

5. FUNDING NUMBERS
C - F41624-96-C-9005
PE - 63723F
PR - 2103
TA - C2
WU - C1

6. AUTHOR(S)
Anthony I. Eller, Raymond C. Cavanagh

7. PERFORMING ORGANIZATION NAME(S) AND ADDRESS(ES)

Science Applications International Corporation
1710 Goodridge Drive
McLean VA 22102

8. PERFORMING ORGANIZATION REPORT NUMBER

9. SPONSORING/MONITORING AGENCY NAME(S) AND ADDRESS(ES)
Air Force Research Laboratory, Human Effectiveness Directorate
Crew System Interface Division
Aural Displays and Bioacoustics Branch
Air Force Materiel Command
Wright-Patterson AFB, OH 45433-7901

10. SPONSORING/MONITORING AGENCY REPORT NUMBER

AFRL-HE-WP-TR-2000-0156

11. SUPPLEMENTARY NOTES

12a. DISTRIBUTION AVAILABILITY STATEMENT

Approved for public release; distribution is unlimited.

12b. DISTRIBUTION CODE

13. ABSTRACT *(Maximum 200 words)*

This is one of five companion reports, each of which deals with one aspect of the problem of assessing the effects of noise from military aircraft on marine life: metrics for sound properties in air compared to sound properties in water; criteria and thresholds for injury and harassment of protected marine life; animal population statistics; and risks of impact from subsonic/supersonic aircraft noise. The purpose of the effort is to establish technically sound estimation procedures for determining the effects of military aircraft noise on marine life, without which the Air Force risks inadvertent violations of the law and becomes vulnerable to litigation and interference with military operations. Objectives include developing procedures for predicting properties of sound waves in air and under water as generated by both subsonic and supersonic aircraft flights; estimating the effects of sound on marine life, both in air and under water; and determining populations of marine life at risk, as functions of aircraft, flight path, and time of year. This volume specifically focuses on the risks of impact to marine mammals from subsonic aircraft noise.

14. SUBJECT TERMS

acoustics, marine animals, noise impacts

15. NUMBER OF PAGES
83

16. PRICE CODE

17. SECURITY CLASSIFICATION OF REPORT	18. SECURITY CLASSIFICATION OF THIS PAGE	19. SECURITY CLASSIFICATION OF ABSTRACT	20. LIMITATION OF ABSTRACT
UNCLASSIFIED	UNCLASSIFIED	UNCLASSIFIED	UL

This page intentionally left blank.

EXECUTIVE SUMMARY

This is one of five companion reports prepared under the sponsorship of Code HECB of the Air Force Research Laboratory (originally funded by Code AL/OEBN, Armstrong Laboratory of Wright-Patterson Air Force Base). Each of the reports deals with one aspect of the problem of assessing the effects of noise from military aircraft on marine life: (I) criteria and thresholds for injury and harassment of protected marine life, (II)/(III) risks of impact from subsonic/supersonic aircraft noise, (IV) metrics for sound properties in air compared to sound properties in water, and (V) animal population statistics.

The end purpose of the multi-year contract effort was to establish technically sound estimation procedures for determining the effects of military aircraft noise on marine life. Without such procedures, the Air Force risks inadvertent violations of the law and becomes vulnerable to litigation and interference with military operations.

Objectives included developing procedures for:
   1) Predicting properties of sound waves in air and under water as generated by both subsonic and supersonic aircraft flights
   2) Estimating the effects of sound on marine life, both in air and under water
   3) Determining populations of marine life at risk, as functions of aircraft, flight path, and time of year.

This volume specifically addresses the approach to bounding the intensity of the noise field in water generated by a subsonic aircraft. Note here that the propagation mechanisms for aircraft noise into water are completely different for sonic booms because of the limited source angle; this is the reason for a separate volume on the subject.

As explained in Section 2, the property of noise in water of interest for risk assessment is the time history of intensity level (or sound pressure level, SPL). Exposure time rules vary among precedents and, just as for impact of noise on humans in the work place, may not be simple energy calculations.

Section 3 reviews, with an annotated bibliography in Appendix A, the well-studied history of propagation from air to water, and aircraft noise in water. It concludes with a recommended, approximate approach for readily estimating bounds on the time series of SPL. Practicality is emphasized, especially in dealing with the rough surface interface and with propagation of the field in water.

Section 4 and Appendix B provide multiple examples for one of the noisier aircraft of concern, the F-18. It shows the time series of the noise in deep and shallow water, and compares the levels to nominal thresholds (starting at the lowest used anywhere to date, 120 dB for long-term exposure). Attention is also paid to the frequency content of the field, since, for example, the majority of marine mammals have very poor hearing at low frequency.

The most important conclusion of this study can be summarized as:

> *For underwater noise generated by subsonic flight of Air Force aircraft, there are very few and limited cases for which there could possibly be any risk to protected marine species of injury or harassment, as determined by commonly used thresholds of today.*

The special cases for which some risk may be present can be determined in advance, and care taken to avoid areas and situations for which protected species may be risk. With attention to such mitigation, compliance concerns for marine life can be all but eliminated.

CONTENTS

This page intentionally left blank.

1.0 INTRODUCTION

1.1 First of Series of Five Reports

This is the second in a series of five companion reports prepared under the sponsorship of the Air Force Research Laboratory (AFRL/HECB), Wright-Patterson Air Force Base (originally sponsored by the Noise Effects Branch, Armstrong Laboratory). Each of the reports deals with one aspect of the problem of assessing the effects of aircraft-generated noise on marine life:

> Report I: Criteria and Thresholds for Adverse Effects of Underwater Noise on Marine Animals

> **Report II: Subsonic Aircraft Noise at and beneath the Ocean Surface: Estimation Models for Metrics Associated with Effects on Marine Mammals**

> Report III: Supersonic Aircraft Noise at and Beneath the Ocean Surface: Estimation Models for Metrics Associated With Effects on Marine Mammals

> Report IV: Background Definitions and Metrics for Sound Properties in Air and in Water Relevant to Noise Effects

> Report V: Marine Animal Populations for Ocean Regions of Interest to Air Force Flight Operations

The end purpose of this multi-year contract effort was to establish technically sound estimation procedures for determining the effects of military aircraft noise on marine life. Without such procedures, the Air Force risks inadvertent violations of the law and becomes vulnerable to litigation and interference with military operations.

Objectives of the contract effort include developing procedures for:
1) Predicting properties of sound waves in air and under water as generated by both subsonic and supersonic aircraft flights
2) Estimating the effects of sound on marine life, both in air and under water
3) Determining populations of marine life at risk, as functions of aircraft, flight path, and time of year.

This volume deals with subsonic aircraft noise.

1.2 Organization of Report and Appendices

Section 2 of this report is intended to provide context and motivation for the effort. In particular, it gives examples of the types of information about the noise field that are needed to assess risk to marine life. Perhaps the most important property common to injury and harassment thresholds for protected species is the dependence on exposure time (both total duration and number of

intermittent events). Estimation of this property (rather than a simple peak SPL or energy metric) is then a target of the effort.

Section 3 contains a review of the literature on the subject of sound propagation from a source in air to a receiver at or below the air-sea interface (Appendix A provides an annotated bibliography for all of the citations). From this review, practical approaches are then recommended for estimating the acoustic field from an aircraft traveling at subsonic speeds. Note that noise from sonic booms has different propagation physics and is covered in a separate report.

Section 4 and Appendix B give a number of examples of the time series of sound pressure level that would be observed at a point in the ocean, as generated by one of the noisier aircraft considered (the F-18).

A conclusion is drawn that it would be a rare event for a subsonic aircraft to generate sufficient noise in water to be considered a source of harassment of protected species, at least for commonly used criteria and thresholds. Furthermore, the approach of this volume, combined with data from companion volumes on criteria/thresholds and on mammal/turtle populations, can be used to identify those cases of concern and afford Air Force the opportunity to greatly limit risk.

1.3 Acknowledgments

2.0 GEOMETRIES AND METRICS OF INTEREST

The purpose of this report is not to advance modeling or data analysis technology of aircraft noise in water, but rather quite specifically to provide approaches and examples of how to predict the properties of aircraft noise in water needed to assess compliance risk. The types of noise properties needed for this problem (risk assessment for non-impulsive noise) have been quite consistent in past compliance documents and in the technical literature. They are relatively easy to characterize – the SPL in a band and the amount of exposure time. Some examples are provided below, to help identify what may be needed and the scales of the problem.

Additionally, treatment of the geometric relationships of the aircraft, the sea surface, and the marine animals is outlined.

2.1 Properties of the Noise Field Needed for Risk Assessment

A companion volume to this report summarizes criteria and thresholds for injury and harassment of protected marine species by underwater noise. Precedents in the eyes of the regulators and other DOD branches (especially Navy and DARPA) must be acknowledged, along with the view of the scientific community.

For non-impulsive, underwater noise (as from a subsonic aircraft overflight or from an underwater projector), injury and harassment thresholds for marine mammals and sea turtles currently used (and likely to be applicable in the future) are almost without exception of the form:

$$\text{THRESHOLD} + A \log \{t\}$$

where THRESHOLD is the sound pressure level (SPL) corresponding to a specified single event or exposure time, and $A \log \{t\}$ is an adjustment for multiple or accumulated exposure time (simply denoted as $\{t\}$). The principal variant on this threshold form is a frequency-band condition, such as application of the rule only for the noise levels in the band below 500 Hz, or the band from 5 kHz to 100 kHz. These bandwidth modifiers generally reflect the hearing band of the species in question, just as A-weighting is used in evaluating noise impact on humans. There is also the complication of special effects thought to be related to low-frequency sound.

The table below provides some relevant examples of thresholds used in recent compliance work. More on this topic can be found in the companion volume to this report dealing with criteria and thresholds for injury and harassment of marine life. All decibel quantities in the table are referred to 1 μPa.

Table 2-1. Examples of Harassment Thresholds

Harassment Criterion	Threshold	Reference
TTS for all small odontocetes exposed to non-impulsive noise at threshold level for corresponding duration	SPL > 192 dB – 17 log T, where T is exposure time in seconds. Exposures counted when time gaps not above dT. Lower threshold limit =120 dB.	Finneran et al. (2000), and NMFS Criteria Workshop (1998)
2.5% of Marine Mammals harassed when exposed to non-impulsive, low-frequency noise above threshold for corresponding duration	SPL > 150 dB – 5 log T, T as above.	SURTASS-LFA DEIS (1999)
50% of Marine Mammals harassed when exposed to non-impulsive, low-frequency noise above threshold for corresponding duration	SPL > 165 dB – 5 log T, T as above.	SURTASS-LFA DEIS (1999)
100% of all Marine Mammals injured for exposures to non-impulsive, low-frequency noise in excess of 180 dB for 30 seconds	SPL > 180 dB	SURTASS-LFA DEIS (1999)
Marine Mammal harassed if exposed to long term noise.	SPL > 160 dB + 10 log D, where D is duty cycle.	LFA EA (1995)

In the first example in the table, the threshold for hearing impact (TTS) for a 1-second exposure of a non-impulsive signal is 192 dB. For a 1-minute exposure, the value is reduced to 162 dB, and for one hour to 132 dB. This is the reason that airplane noise must be addressed with care. If this type of threshold were to be used, hovering helicopters and circling fixed wing aircraft may be judged as problematic.

To avoid risk or to show that there is no impact, estimates are needed of the time series of noise as received by the animal. It is not enough to estimate maximum levels, but rather the total number of exposure intervals for a given time window.

This paper then provides approaches for estimating these exposure values in the water for the case of subsonic aircraft sources.

Note that for impulsive noise (such as sonic booms), the most commonly used thresholds for injury and harassment are based on a completely different set of noise metrics (such as peak pressure, positive impulse, energy flux density) from SPL. This topic is addressed in a companion volume on impulsive noise.

2.2 Animal/Interface/Aircraft Geometries

In assessing risk of injury or harassment of protected species, the key elements are the time history of the noise at a site in the ocean (as outlined above) and the movement of the animals of concern. The former is a function of aircraft source level, speed, altitude, and lateral distance, as well as of the propagation environment in air and in water. At each point in the ocean, the time series can be estimated, and the impact assessed. Statistical descriptions of animal populations are then applied to determine the likelihood of encounter.

For long exposure potentials, as in the case of a hovering helicopter, animal motion most also be addressed. The problem often comes down to one of determining the chances that an animal will stay within an area for a specific amount of time (e.g., within 1 km of the helicopter for one hour). Rather than address the animal motion problem here (it takes many pages), we can only alert the planner to the problem, and note that several methods of solution have been used in the past (see, for example, Standard EIGER I EA (1995) and SURTASS-LFA DEIS (1999)).

The usual approach to risk estimation for moving sources and exposure-time-dependent thresholds for injury/harassment is to map out the ocean region consisting of all locations ensonified at or above threshold levels. The expected number of animals affected is then the size of that ensonified region multiplied by animal density. The ensonified region is usually characterized in terms of area, and terms such as 'footprint' or 'sweep region' are sometimes used. If there is a bias for the ensonification and animal location in depth, then the appropriate volume of the region and revised animal densities must be considered.

As an illustrative example, suppose and aircraft ensonifies the ocean region within 1000 m on either side, to depths of 1000 m, at threshold levels (e.g., SPL above 140 dB for 20 seconds). If the aircraft follows a non-overlapping path for one hour at 200 km/hr, then the impact region would have area of 200 km^2. If the density of blue whales was 0.0004/km^2, then the expected number of blue whales to be affected would be about 0.08, well below what would ordinarily be considered a significant risk.

3.0 NOISE ESTIMATION

This section addresses the estimation of the acoustic field resulting from the transmission of sound from subsonic moving noise sources in air into the ocean below. Interest in this problem arises primarily from two applications: (1) detecting the presence of aircraft by submerged sensors, which interest has motivated most of the research and measurements for this problem, and (2) estimating the possible impact of noise on the biological environment. The latter is the motivation for this report and addresses the concern that the noise from loud, or even moderately loud, aircraft can reach levels in water below the flight path that are sufficiently great to have biologically significant impact on marine life. This paper recommends schemes to estimate the time-dependent pressure levels in water that would be heard by a marine animal. The approach is based on theory and data from the scientific literature, and examples show representative predictions of the depth and lateral displacement where received levels exceed a nominal harassment threshold.

3.1 Physics Overview: Understanding the Basic Problem

A noise source moves at subsonic speed above water, and our ultimate interest is to determine the resulting sound level in the water, both in regions more or less directly beneath the sound source as well as in regions having substantial lateral displacement from the source. The problem divides naturally into three domains: 1) propagation of noise from the source through the air to the air-water interface, 2) transmission of part of the pressure field across the interface into the water, and 3) propagation, possibly to great distances, in the water. As long as the source motion is slower than the sound speed in air, then details of the motion itself do not influence the transmission of the pressure field into the water, and for convenience the noise source may be regarded as stationary. The motion of the source will cause a perceived shift in the frequency of the noise signal, but this effect is not important for estimating the sound pressure level. For a great many applications the controlling physics is that associated with transmission through the air-water interface. That aspect of the problem will be outlined in qualitative terms before we begin a more detailed description of the entire problem.

The geometry is illustrated in Figure 3.1-1. Ray path language will be used to describe the basic mechanisms for purposes of this overview, and a more rigorous discussion of the physics will be presented in later sections. A noise source is located at some height above the water and radiates in all directions. Ray paths from the source that strike the air-water surface within an approximately 13-degree cone about the vertical enter the water and propagate at a refracted angle that is greater than the incidence angle, measured from the vertical. These paths are the direct transmission paths. All points in the water can be reached by direct transmission paths, and these are the strongest and generally most important transmission paths in the context of the present discussion. Paths A and B in Figure 3.1-1 are examples of direct transmission paths.

Ray paths in air that lie outside the 13-degree cone, path C for example in Figure 3.1-1, do not propagate directly into the water when they strike the air-water interface. A pressure field is created in the water, but it dies out rapidly with increasing depth and is confined to a thin "skin" depth just beneath the water surface. This field is generally referred to as an evanescent field. Water points located beneath the 13-degree cone, such as point #1 in Figure 3.1-1, receive only a

direct transmission signal. Water points outside the region beneath the critical cone, however, such as point #2 in Figure 3.1-1, receive a signal along a direct transmission path (path B) as well as an evanescent path (path C). The direct field becomes small as the field point #2 approaches the surface, and the evanescent field is significant only near the surface.

A third contribution to the received pressure field is the result of energy that is scattered, or redirected, in the forward direction as it passes through the rough air-water interface. As a result the noise signal arrives at the receiving field point along a spread of vertical angles in addition to the specular path related to a flat interface. There is not general consensus in the scientific community about how to account for these contributions. Many papers view the scattered path as geometrical transmission through a locally flat but tilted portion of the interface; other papers account as well for the limited size of the locally tilted facet, as compared to the wavelength, which causes additional angle spreading of the signal from the facet. The scattered field is generally important only in the sense that it redirects the pressure field into the near surface region, outside the region directly beneath the critical cone, and tends to fill in where the direct transmission is small. Thus, large effects of scattering are reported in the sense that a measurable signal is found in a region that would otherwise be in a shadow.

The above discussion is based on the convenient assumption that the sound speed structure in the air is uniform so that the sound in air propagates along straight paths. In many cases, when the air temperature varies substantially with depth or when there is significant wind, that will not be the case, and the area at the surface of the critical cone may be either larger or smaller, depending on conditions. Similarly, actual water sound speeds and the presence of the ocean bottom may create long range propagation paths that can be excited, allowing the sound to extend to much greater lateral positions than otherwise possible.

In the case of weak sound sources or of sources at great altitude above the water, the expected sound levels in the water will be of significant strength only in the regions close to directly beneath the source, with little lateral separation. Propagation through the air is close to the vertical direction and not greatly influenced by details of the sound speed structure in the air. In contrast, loud sources in air may have a substantial lateral component and be subject to many of the details in the sound speed profiles both in air and water.
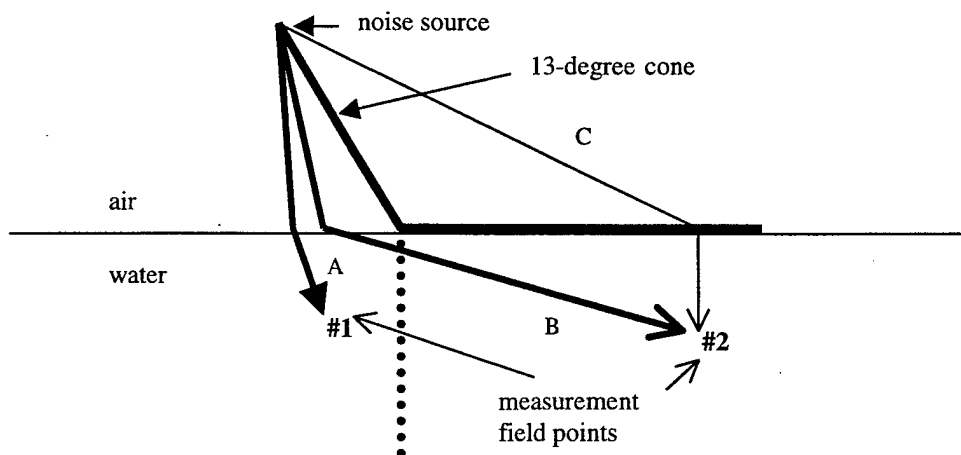

Figure 3.1-1. Geometry of the problem.

3.2 Physical Mechanisms: Transmission across the Air-Water Interface

3.2.1 Plane Wave Transmission from Air to Water -- Incidence Angles Less than Critical

The acoustic pressure field in the water, for a plane wave in air with an incidence angle less than $\arcsin(c_1/c_2)$, or within about 13 degrees of normal incidence, is a plane wave propagating in the water at a lower incidence angle related to the initial angle by

$$\sin \theta_2 = (c_2/c_1) \sin \theta_1 \qquad (1)$$

where c_1 and c_2 are the sound speeds in air and water, respectively, and θ_1 and θ_2 are the angles of incidence, measured from the vertical, in each medium as depicted in Figure 3.2-1. Typical values of sound speed are 343 m/sec in air and 1500 m/sec in water. The ratio T (pressure transmission ratio) of the pressure amplitude P_{2pw} of a plane wave in the water to the amplitude P_{1pw} of an incoming plane wave in air is

$$P_{2pw}/P_{1pw} = T = 2 \rho_2 c_2 \cos \theta_1 / [\rho_2 c_2 \cos \theta_1 + \rho_1 c_1 \cos \theta_2], \qquad (2)$$

or $\qquad\qquad\qquad T = 2 / (1 + \varepsilon),$

where $\varepsilon = (\rho_1 c_1 \cos \theta_2 / \rho_2 c_2 \cos \theta_1)$ and ρ_1, ρ_2 are the densities of air and water. For transmission from air to water ε has values less than about 0.0003, and T may be approximated as 2 in all practical calculations. The term *amplitude* is used here to indicate the rms amplitude rather than a sinusoidal peak value.

3.2.2 Plane Wave Transmission from Air to Water – Incidence Angles Greater than Critical

For an incident single frequency plane wave of amplitude P_{1pw} in air propagating in the x-z plane and with an incidence angle greater than critical, the pressure $p_2(x,z,t)$ in water is described by

$$p_2 (x,z,t) = T P_{1pw} \exp(- 2\pi \gamma z/\lambda_2) \exp[j \omega (t-(x/c_1)\sin \theta_1)], \qquad (3)$$

where λ_2 is the wavelength in water, and T is the pressure transmission ratio at the interface, given by

$$T = 2 \cos\{\arctan [(\rho_1 c_1 / \rho_2 c_2)(\gamma/\cos\theta_1)]\}, \qquad (4)$$

and $\qquad \gamma = [(c_2/c_1)^2\sin^2\theta_1 - 1]^{1/2}. \qquad (5)$

These equations represent a pressure field with vertical phase fronts moving along the x-direction and decaying exponentially as one moves vertically downward in water. This is known as an evanescent field. Acoustic energy in the water propagates along the x-direction close to the interface and does not propagate downward into the water. The value of the pressure

transmission ratio T is approximately 2 for all incidence angles except those within a fraction of a degree of a horizontal grazing ray. The evanescent decay rate with depth is given by

$$20 \log \{p_2 (x,z_a,t)/p_2 (x,z_b,t)\} = (8.7) \, 2\pi \, \gamma \, [z_a - z_b \,]/\lambda_2 \, dB = (8.7) \, 2\pi \, \gamma \, dB \text{ per wavelength}$$

This quantity gives the decay with distance below the interface and is presented in Figure 3.2-2.

3.2.3 Transmission into Water from a Point Source in Air

The mathematical treatment of radiation from a point source in one medium and transmission of the field into a second medium is a fundamental problem in acoustics and, earlier, in electromagnetic theory. Early treatments were published by Sommerfeld and later by Weyl and are summarized in the classic text by Stratton (1941). (References are listed in the Bibliography and described further in the Annotated Bibliography Appendix.) The paper by Gerjuoy (1948) is perhaps the earliest scientific treatment of this particular problem, transmission from a slow medium into a faster medium, available in the English language and is a good example of how even this simplified problem can pose a mathematical challenge at an advanced level.

This problem has been examined both from a wave as well as a ray viewpoint. A primary finding [Gerjuoy (1948) and Chapman and Ward (1990)] is that both sets of results, wave and ray, agree in a high frequency limit and support the interpretation presented in the overiew that any point in the water directly below the critical angle cone receives only directly transmitted energy, and a point in the water outside the critical angle receives both the directly transmitted energy and an exponentially decaying (evanescent) term. For the present application of a source in air over water, Gerjuoy states that at field points near the surface and sufficiently outside the critical angle, the exponentially decaying term is greater than the directly transmitted pressure.

Gerjuoy presents a detailed examination of contour integration related to the wave approach. He obtains asymptotic expressions for the infinite integrals by application of the method of steepest descents and obtains results for the directly transmitted field that are identical with ray tracing results. The asymptotic solution also gives an evanescent field at locations not beneath the critical angle cone.

The ray trace result for direct transmission, as given by Pierce (1981), is

$$P_2 / P_1 = \frac{2 \cos \theta_1}{[h + d(c_2/c_1) (1/B)]^{1/2} \; [h + d(c_2/c_1) (1/B^3)]^{1/2}} \quad (6)$$

where $B = \cos \theta_2/\cos \theta_1$. $\quad (7)$

B takes values between 0 and 1. The value B = 1 corresponds to sound reception directly beneath the source with θ_1 and θ_2 both equal to zero, and for this case one has

$$P_2 / P_1 = \frac{2}{[\, h + d(c_2/c_1)\,]} \, . \tag{8}$$

The other limit, $B = 0$, corresponds to the horizontal ray path that grazes the surface when the incidence angle in air equals the critical angle. As $\cos \theta_2$ approaches zero at large lateral distance from the critical region one has

$$P_2 / P_1 \rightarrow (2/R)\,(c_1/c_2)\,(\cos \theta_2/\cos \theta_c), \tag{9}$$

which approaches zero at the interface, and where R is the slant distance from the measurement point to the point where the incident ray crosses the interface. It is noted that the dipole angular dependence exhibited here is a result entirely of the divergence of neighboring rays near the surface and is not a result of the pressure release condition as seen from the water side of the interface. Ray theory itself does not acknowledge the pressure release boundary condition.

Contrary to the ray-theoretic approach, which predicts zero amplitude at the surface outside the critical zone, wave-theoretic results indicate that the field has finite value at the surface and gives rise to the lateral wave observed in air.
Simplified, easier to compute expressions for the ray theoretic prediction of the directly transmitted field into the water from a point source in air are available, also. Young (1971,1973), for example, gives the simplified form

$$P_2 / P_1 = [(2c_1/c_2)\,\cos \theta_2]\,/r \, , \tag{10}$$

where r is the distance indicated in Figure 3.2-3a. Young's result has the physical interpretation that the field in water is computed as though it came from a dipole source located at a reduced altitude $h' = (c_1/c_2)\, h$, and has a source level changed by $20 \log(2c_1/c_2)$, or a reduction of about 6.8 dB.

Urick (1972) presents the same result, Eq. (10), but with the geometry shown in Figure 3.2-3b. The effective dipole source now is located at the sea surface and, as for the Young result, has a source level reduced by 6.8 dB, in addition to any further reductions by sound absorption in air. The range r is the distance from the measurement point to the point on the interface directly below the source in air. Urick stipulates further that this is a far field result, valid at lateral ranges much greater than the height of the actual source. One may note the curiosity that, other than this stipulation of being at ranges greater than the source height, Urick's result has no explicit dependence on source height.

The Young and Urick results offer a convenience of insight into the dipole nature of the field and quick calculation, but they fail to delineate the actual field structure at closer distances.

3-5

3.2.4 Effects of scattering by the rough air-water interface

A consensus interpretation of the several papers that address scattering from the rough interface is that (1) the ocean surface can be pictured as consisting of a collection of locally flat facets tilted from the vertical according to a probabilistic distribution, and (2) transmission through each tilted facet occurs at the proper Snell angle as though the facet were of infinite extent. A summary of results indicates that the primary effect of rough surface scattering on the transmission of sound across the air water interface is to partially fill in the shadow region close to the surface and laterally distant from the critical region. No significant effect is reported for transmission at near normal incidence.

These results may be integrated into earlier results by the following equation synthesized from results presented by Lubard and Hurdle (1976)

$$P_2/P_1 = (2/R)\,(c_1/c_2)\,\sin\,(\phi^2 + <\alpha^2>)^{1/2}. \tag{11}$$

where R is the distance from measurement point to the point where the direct path crosses the interface, and α is the angle of a facet on the rough sea surface, measured from the vertical. Variables are defined as in Figure A3 in Appendix A, the Annotated Bibliography.
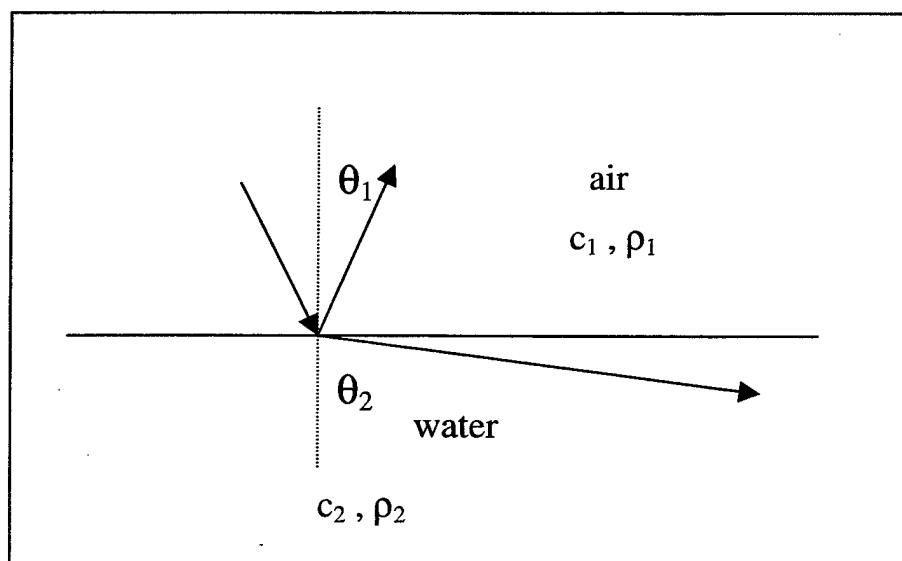

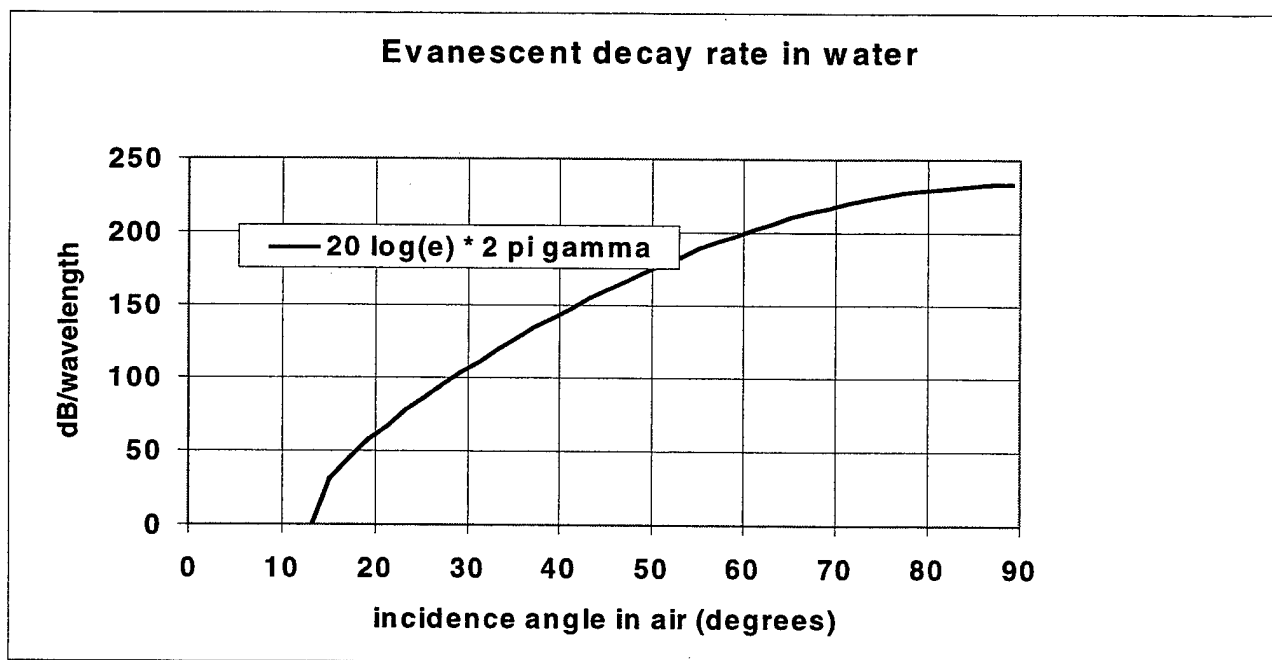Figure 3.2-1. Geometry for plane wave transmission from air into water

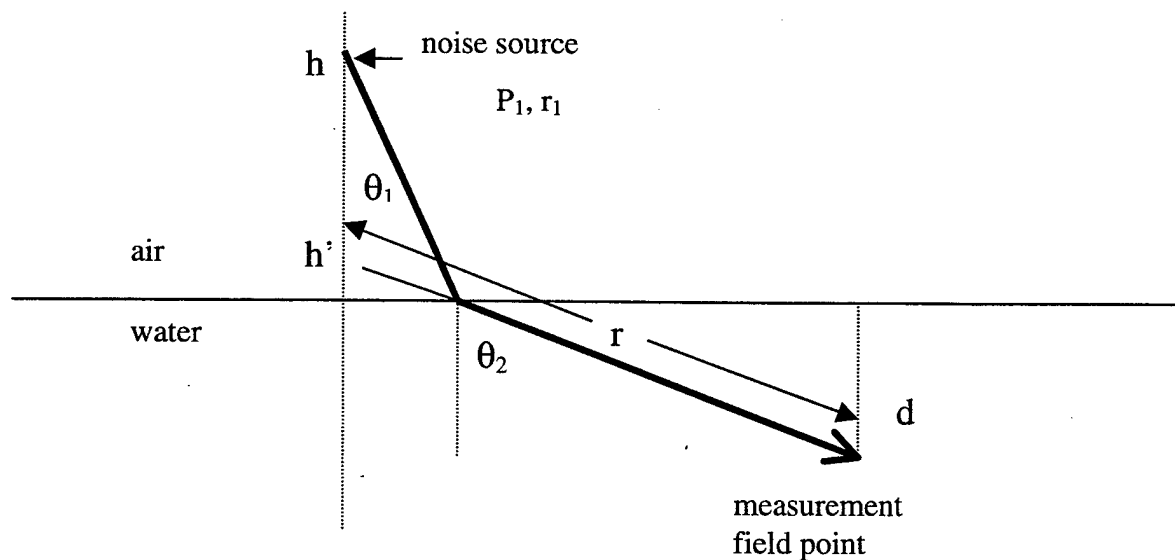Figure 3.2-2. Evanescent decay rate with depth in water

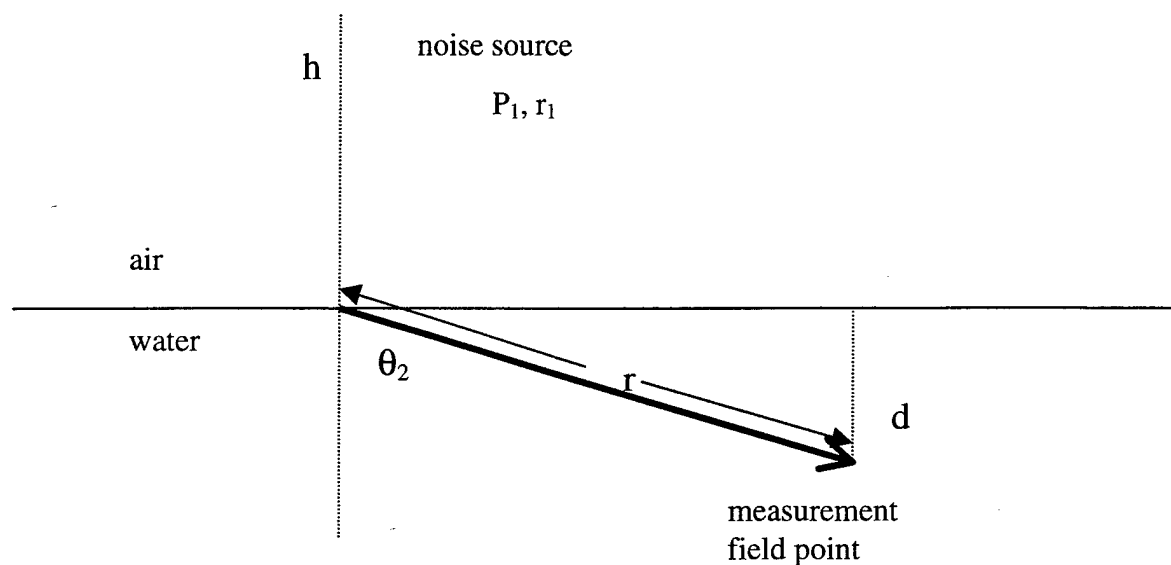Figure 3.2-3a. Geometry used by Young. The effective dipole source is placed at height h'.

Figure 3.2-3b. Geometry used by Urick. The effective dipole source is placed at the air-water interface.

3.3 Aircraft Noise Source Levels and Propagation in Air

3.3.1 Use of Decibels and Reference Pressures

This section deals with measures of aircraft noise. By convention the term *level* is used to indicate that a quantity is expressed in decibels, dB. Acoustic noise levels, expressed in dB, are defined as 10 times the logarithm to base 10 of the ratio of the mean square pressure to the square of a reference pressure. Again by convention, the reference sound pressure used when determining pressure levels of signals in air is 20 µPa. On the other hand, sound pressure levels in water are expressed in reference to 1 µPa. In this report the final interest is to determine values of sound pressure level (SPL) in water. Thus, to minimize confusion, all measures of noise level will be stated with reference to 1 µPa.

To convert an SPL from one reference to the other, note that

$$X \text{ dB (re 1 µPa)} = (X - 26) \text{ dB (re 20 µPa)}.$$

For example,
$$150 \text{ dB (re 1 µPa)} = 124 \text{ dB (re 20 µPa)}.$$

Note also that estimates of the field are made in terms of pressure level, which has no reference to impedance in its definition. Absolute intensities can be estimated under the plane wave

assumption from pressure and impedance, but there is no need for the added confusion in this report.

3.3.2 Noise Band and Spectrum Levels

Representative levels and spectral characteristics of radiated noise from military aircraft were taken from published Air Force data bases (e.g., OMEGA 10, ASAN). This noise source 'model' consists of two sets of data for three representative aircraft (covering a range of aircraft of radiation levels). The first set of data provided by the model is the normalized sound pressure level at a nominal distance of 1000 ft in standard one-third octave bands. The other set of data is the total level, accumulated over all one-third-octave bands, presented as a function of distance from the source. These two sets of data, with a slight adjustment to make them consistent, were used to determine aircraft source levels whose values were subsequently used to predict underwater levels for actual aircraft. This is intended to demonstrate the steps that are taken for any aircraft to estimate impact. The aircraft noise source level in this report is defined as the sound pressure level when extrapolated to a reference distance from the source, taken here as 1 m. (source level, of course, depends on direction as provided in the data bases).

Three representative examples of noise levels computed by this model are presented in Table 3.3-1. This table presents sound pressure levels in successive one-third-octave bands, each band identified by its geometric center frequency. The center frequencies shown here, 50 Hz through 10,000 Hz, are standard center frequencies used in presenting noise data. A one-third-octave spectral band has a bandwidth equal to about 1.23 times (or about 23% of) the center frequency. Although the original data sets provided values in dB **re** 20 µPa, the standard reference in air, all values in Table 3.3-1 have been increased by 26 dB to convert them to dB **re** 1 µPa. The other information presented in the table is the one-third-octave band source level, that is, the band level extrapolated back toward the source to a reference position of 1 m.

The total sound level for all 24 bands presented is computed by converting the level in each band to the corresponding intensity value, summing the 24 intensity values, and finally converting the total back to a dB level. · Values of band level are presented for three different bands: (a) the total band consisting of all 24 third octave bands from 50 to 10000 Hz, (b) a low frequency band from 50 to 2000 Hz and (c) a high frequency band from 2000 to 10000 Hz. These same band levels are plotted for all three aircraft in Figure 3.3-1

Another commonly used measure for noise levels is the spectrum level, in which the above information is presented in terms of the energy in a 1-Hz band, instead of a one-third-octave band. The spectrum levels, evaluated at the 1/3-octave band center frequencies for the E-8A aircraft, are compared to the 1/3-octave-band levels in Figure 3.3-2. At each of the center frequencies, the spectrum level is always lower than the corresponding one-third-octave band level, and the size of the difference is proportional to frequency [$10 \log (0.23f)$ or about $10 \log f - 6$ dB, for f the center frequency in Hz].

3-9
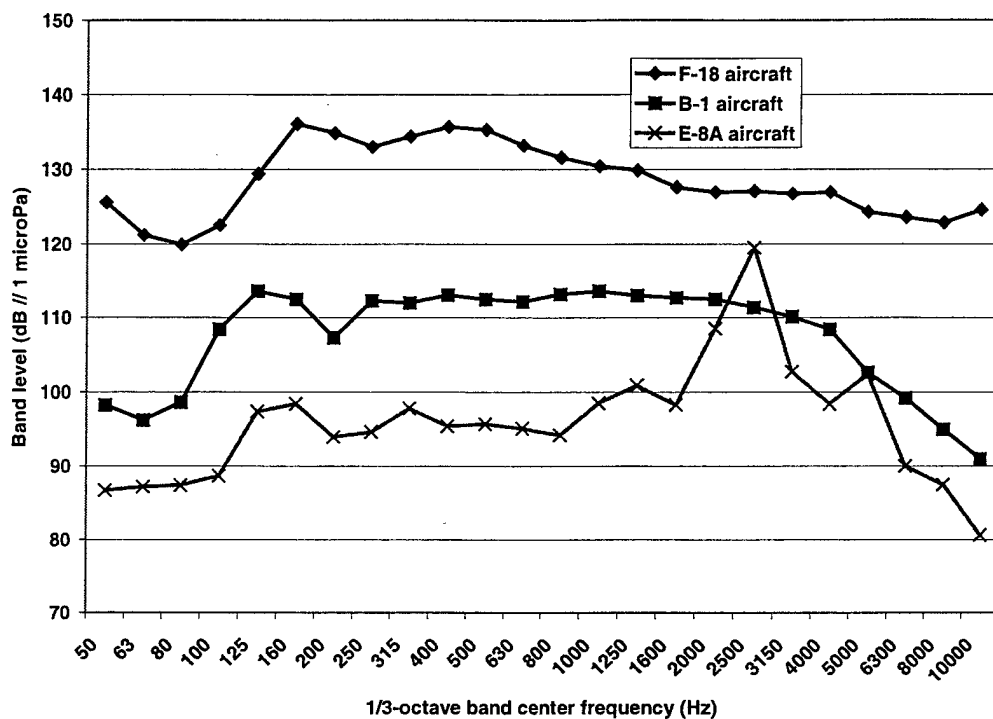
Figure 3.3-1. One-third octave band sound pressure levels at nominal slant distance of 1000 ft for three aircraft. (Data from Table 3.3-1)

Table 3.3-2. Standard A-weighting

Frequency (Hz)	A-weights (dB)	Frequency (Hz)	A-weights (Hz)
50	-30.2	800	-0.8
63	-26.2	1000	0.0
80	-22.5	1250	0.6
100	-19.1	1600	1.0
125	-16.1	2000	1.2
160	-13.4	2500	1.3
200	-10.9	3150	1.2
250	-8.6	4000	1.0
315	-6.6	5000	0.5
400	-4.8	6300	-0.1
500	-3.2	8000	-1.1
630	-1.9	10000	-2.5

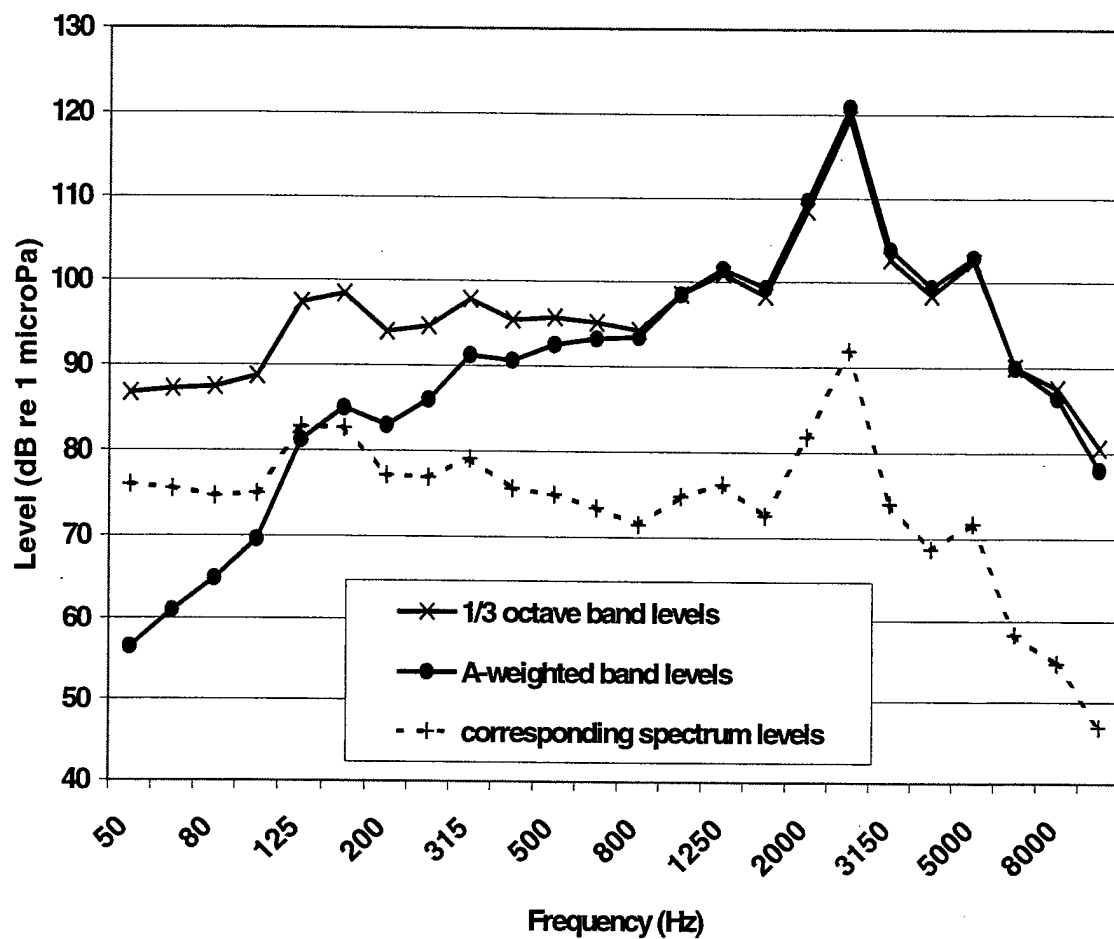Figure 3.3-2 Comparison of 1/3-octave band, spectrum, and A-weighted 1/3-octave band levels for E-8A aircraft during flight operations.

Table 3.3-1. One-third-octave band sound pressure levels at a nominal range of 1000 ft for three aircraft and one-third-octave band source levels (range of 1 m).

center ,frequency (Hz)	F-18 aircraft airspeed 250 knots		B-1 aircraft airspeed 360 knots		E-8A aircraft airspeed 250 knots	
	1/3 octave band level (dB re 1μPa)	1/3 octave band source level (dB re 1μPa @ 1m)	1/3 octave band level (dB re 1μPa)	1/3 octave band source level (dB re 1μPa @ 1m)	1/3 octave band level (dB re 1μPa)	1/3 octave band source level (dB re 1μPa @ 1m)
50	125.6	177.3	98.2	150.4	86.7	138.7
63	121.2	172.9	96.2	148.4	87.2	139.2
80	119.9	171.6	98.6	150.9	87.4	139.4
100	122.5	174.2	108.4	160.7	88.7	140.8
125	129.4	181.2	113.6	166.0	97.4	149.5
160	136.1	188.0	112.5	165.0	98.4	150.6
200	134.9	186.9	107.3	159.9	93.9	146.2
250	133.0	185.1	112.3	165.0	94.6	147.1
315	134.4	186.6	112.0	164.8	97.8	150.4
400	135.7	188.1	113.1	166.1	95.4	148.1
500	135.3	187.8	112.5	165.6	95.7	148.6
630	133.2	185.8	112.2	165.4	95.1	148.1
800	131.6	184.3	113.2	166.6	94.2	147.3
1000	130.4	183.3	113.6	167.1	98.5	151.8
1250	129.9	183.0	113.0	166.7	100.9	154.4
1600	127.6	181.0	112.7	166.7	98.3	152.1
2000	126.9	180.7	112.5	167.0	108.5	162.7
2500	127.1	181.5	111.4	166.6	119.5	174.4
3150	126.7	182.2	110.1	166.4	102.7	158.7
4000	126.9	184.1	108.4	166.5	98.4	156.2
5000	124.3	184.0	102.6	163.4	102.4	162.8
6300	123.6	187.4	99.2	164.4	90.0	154.7
8000	122.9	193.5	95.0	167.4	87.5	159.2
10000	124.6	205.1	91.0	174.0	80.6	162.6
Total band level for all 24 bands	144.7	206.1	124.4	180.0	120.3	175.6
Band level for bands from 50 to 2000 Hz	144.4	196.7	123.8	177.1	111.3	165.0
Band level for bands from 2000 to 10000 Hz	141.0	205.8	122.3	179.1	120.2	175.6

3-12

Yet another approach to characterize noise, appropriate primarily for noise as perceived by humans, is to weight each part of the spectrum according to the hearing threshold of the human ear. The weightings used in this process are presented in Table 3.3-2, and the resulting "A-weighted" one-third-octave band levels are included in Figure 3.3-2. Levels at the low and high frequency ends of the spectrum are decreased, while bands from 1000 to 5000 Hz are increased slightly. The total band level, obtained by converting dB levels to the corresponding intensity, summing the intensities for all bands and then converting the result to decibels, is 95.7 dBA. The term "dBA" is used to indicate that the levels have been A-weighted.

3.3.3 Determination of Noise One-Third-Octave Band Source Levels

This section addresses how to extrapolate model results for the noise spectrum and dependence on distance in order to estimate noise source levels in 1/3-octave band at a reference range of 1 meter. This goal is accomplished by computing the expected acoustic losses as a function of range and frequency, and then using the results to predict the levels at 1 m. Aircraft source model output for noise level against range will be used to validate the source level estimates.

3.3.4 Spreading and Absorption Losses

Signals propagating in air from a source to a distant location will decrease in level by spherical spreading, as the signal energy spreads out in all directions, and by energy absorption. For nearly all situations of interest in the present application, these two mechanisms suffice to relate the sound pressure level at any location to its value at some reference point near the source. Thus the sound pressure level of sound at frequency f and range r from the source is specified by

$$SPL(r,f) = SPL(r_1,f) - 20 \log(r/r_1) - \alpha(f)(r - r_1), \qquad (12)$$

where r_1 is a reference distance from the source, $\alpha(f)$ is the frequency dependent absorption coefficient and $SPL(r_1,f)$ is the pressure level at specified range and frequency. The absorption coefficient in air for audio frequencies is due almost entirely to multiple molecular thermal relaxations, and the value is sensitive to both temperature and humidity. The so-called classical absorption mechanisms of shear viscosity and thermal conductivity are relatively unimportant in air under conditions of interest here.

Representative values of $\alpha(f)$ were computed on the basis of Eq. (13) in the paper by Bass et. al. [Bass, Bauer and Evans, 1972]. Values used for A_i and T_i (i = 1 - 3) are based on Eq. (14) in that paper. Values for T_4 and c are $T_4 = 5 \times 10^{-10}$ and c = 1.13 kft/s (equivalent to 344.4 m/s) as indicated in the paper. This set of equations gives computed values of α as a function of humidity and for 20°C. The dependence of absorption on humidity is relatively weak over the span of humidities expected over the ocean. Computed values of α for humidities of 50%, 75% and 100% are compared in Figure 3.3-3. Corresponding values of absorption in sea-water [Urick, 1967, p.92] are presented also, and it is apparent that the absorption losses are far less in water than over the same distances in air. The results from the aircraft source model were based on a humidity of 70% and a temperature of 59°F (15°C). Values for α, given in dB/m at each

3-13

standard 1/3-octave-band center frequency, and corresponding to a humidity of 70% and temperature of 20 °C, were computed and are presented in Table 3.3-3.

3.3.4 Noise as a function of distance

The propagation loss at a single frequency, or approximately for a one-third octave band, then is specified by the geometric (spherical) spreading and by the frequency dependent absorption loss that is proportional to range. Representative curves of SPL against range are shown for selected frequencies in Figure 3.3-4. In each case the sound pressure level at 1 m is given as 0 dB. This figure shows that the high frequency components become dominated by absorption losses within 1000 m from the source. A curve for spherical spreading without absorption is shown as well.

Table 3.3-3. Atmospheric absorption at 1/3-octave-band center frequencies for a temperature of 20°C and humidity of 70%.

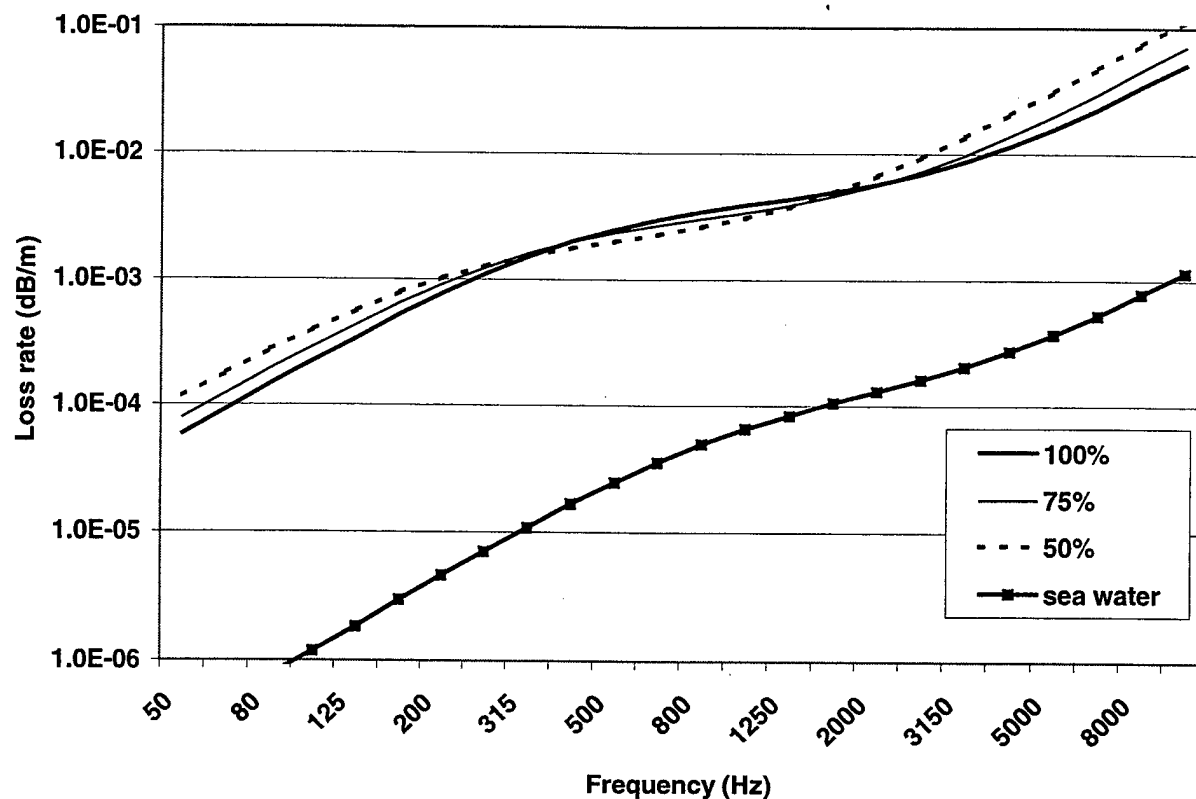| Frequency (Hz)	Absorption (db/km)	Frequency (Hz)	Absorption (db/km)
50	0.08	1000	3.3
63	0.1	1250	3.8
80	0.2	1600	4.6
100	0.3	2000	5.7
160	0.5	2500	7.4
200	0.7	3150	10.2
250	0.9	4000	14.7
315	1.2	5000	21.3
400	2.0	6300	32.2
500	2.3	8000	50.0
630	2.6	10000	76.0
800	2.9		

Figure 3.3-3 Dependence of atmospheric absorption on frequency and humidity for a temperature of 20°C.   Sea-water absorption is shown also.
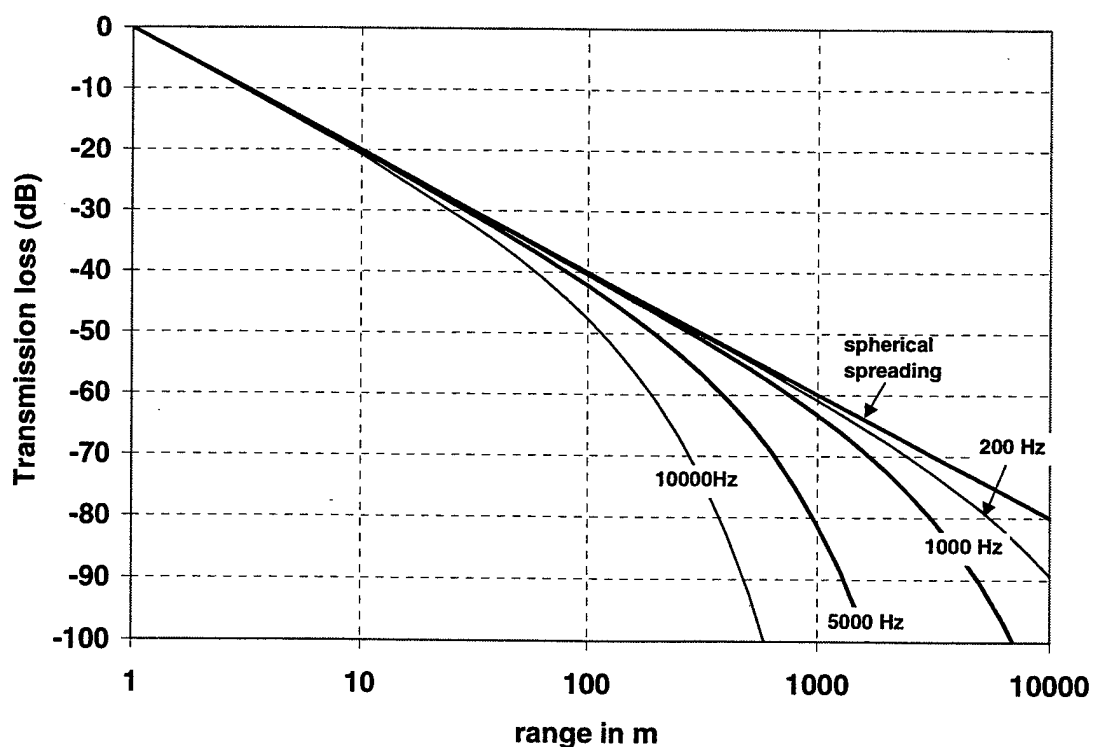

Figure 3.3-4. Single frequency propagation loss against range from spreading and absorption

3-15

Outputs of the noise source model include total noise level (assumed to mean over the entire set of 24 1/3-octave bands from 50 to 10000 Hz) as a function of distance. Model output values for SPL for the three aircraft selected are presented at logarithmic ranges in Table 3.3-4. Results from the Aircraft source model are identified as Sound Exposure Level (SEL). For continuous, as compared to transient, noises this is the same as SPL.

Table 3.3-4 Model results for SPL
vs range for three aircraft.

Distance	F-18	B-1	E-8A
(m)	(dB re 1uPa)	(dB re 1uPa)	(dB re 1uPa)
61.0	164.0	139.6	136.7
76.2	161.5	137.9	135.0
96.0	159.0	136.2	133.3
121.9	156.4	134.5	131.5
152.4	153.8	132.7	129.6
192.0	151.3	130.9	127.6
243.8	149.0	129.0	125.5
304.8	146.8	127.0	123.2
381.0	144.7	124.9	120.7
487.7	142.7	122.8	117.9
609.6	140.6	120.5	114.7
762.0	138.5	118.1	111.1
960.1	136.3	115.6	107.1
1219.1	134.0	113.0	102.4
1523.9	131.6	110.3	97.3
1920.1	129.1	107.4	91.8
2438.3	126.4	104.3	86.6
3047.9	123.5	101.1	82.3
3809.8	120.4	97.7	78.5
4876.6	117.0	94.2	75.0
6095.7	113.4	90.5	71.4
7619.6	109.6	86.7	67.7

Using the propagation model defined by Eq. 12 along with the frequency dependent absorption values in Table 3.3-3 and the 1/3-octave-band levels in Table 3.3-1, values of SPL were computed for each of the three aircraft over all frequencies and ranges. Total band level (over all 24 bands) were also determined by summing over the frequency bands as a function of range. The results computed by this approach are presented in Figures 3.3-5 through 3.3-7, represented by the solid curve as marked, and the level-vs-range data provided by the Aircraft source model are presented by the data markers. There are three reasons for making this comparison: First, the generally consistent agreement between the curves and data markers serves to validate the computational approach represented by Eq. 12. Second, this gives us a means of determining

3-16

21

results for separate frequency bands, not always available in the radiated noise data bases. Third, the results provide an estimate of the effective aircraft source level, extrapolated to 1 m, as a function of frequency.

Sound pressure levels for wide band signals behave differently than the single frequency curves in Figure 3.3-4. The shape of the curves is controlled by the shape of the spectrum. The high frequency contributions decay rapidly, leaving the lower frequency bands at long range. The spherical spreading curve is presented in each figure also. Departure from this curve indicates the importance of the absorption in each case.

3.3.6 Influences of sound speed profile structure

The above description of propagation loss in the atmosphere is based on an implicit assumption that the sound speed is uniform in space and that, consequently, the energy propagates along straight line paths. In reality, sound speed profiles are sensitive to altitude and to lesser extent, to lateral position. Representative sound speed profiles for summer and winter [Pierce (1981) p. 395] show a sound speed that decreases with increasing altitude at an approximately constant rate on the order of -0.006 sec^{-1}.

A result of this sound speed structure is that rays heading downward form the source will refract outward. This has two consequences. First, the rays reaching the water interface at the critical incidence angle will leave the source at a slightly smaller angle, and the lateral extent of the critical cone as it intersects the water surface will be slightly smaller that it would for a uniform sound speed. Second, there will be no direct ray from the source in air to the water interface at large lateral separations. The presence of wind can further influence the propagation. Preliminary calculations to quantify these effects showed that their influence is very small in the context of the present application, and no further consideration is made here.
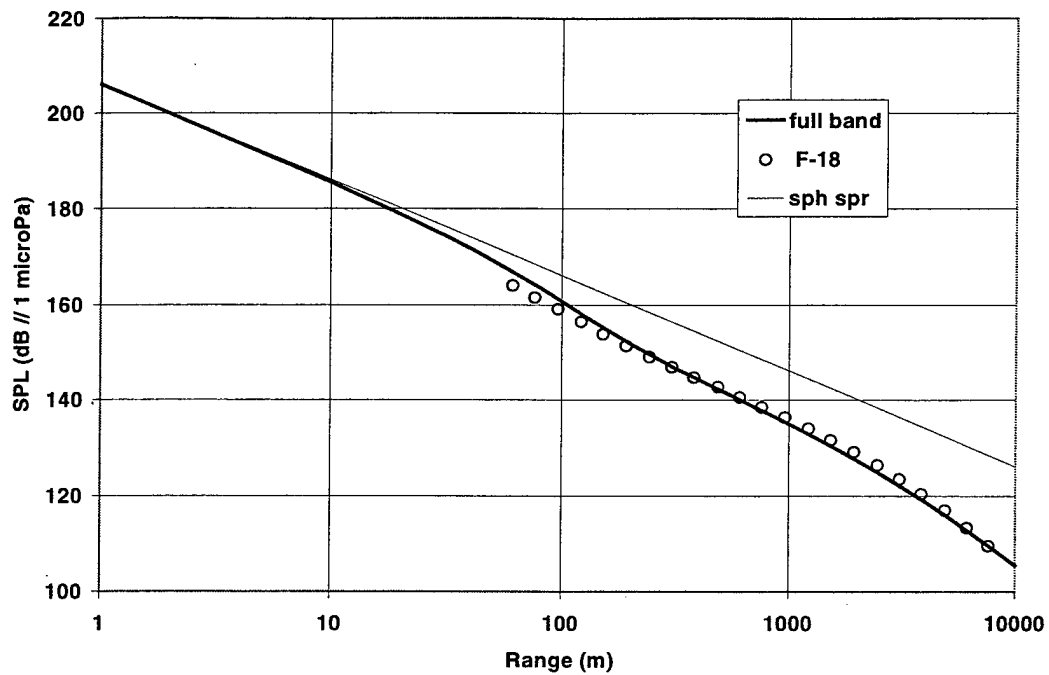
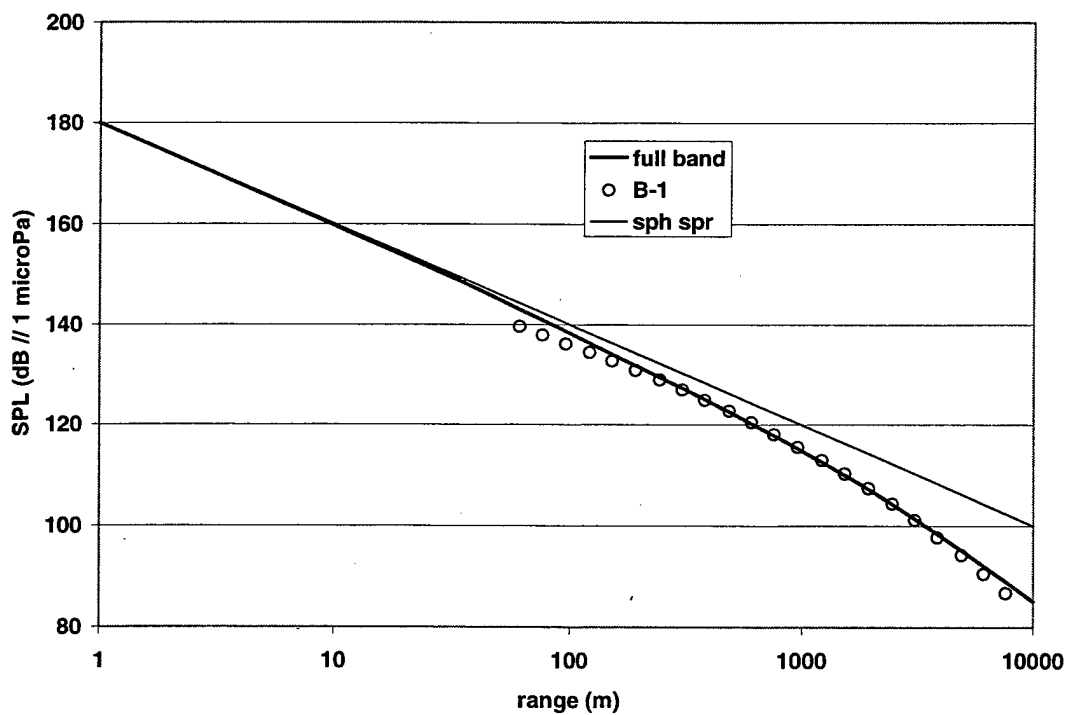Figure 3.3-5. Full-band propagation sound pressure level for F-18 aircraft as a function of distance.

Figure 3.3-6 Full-band propagation sound pressure level for B-1 aircraft as a function of distance.
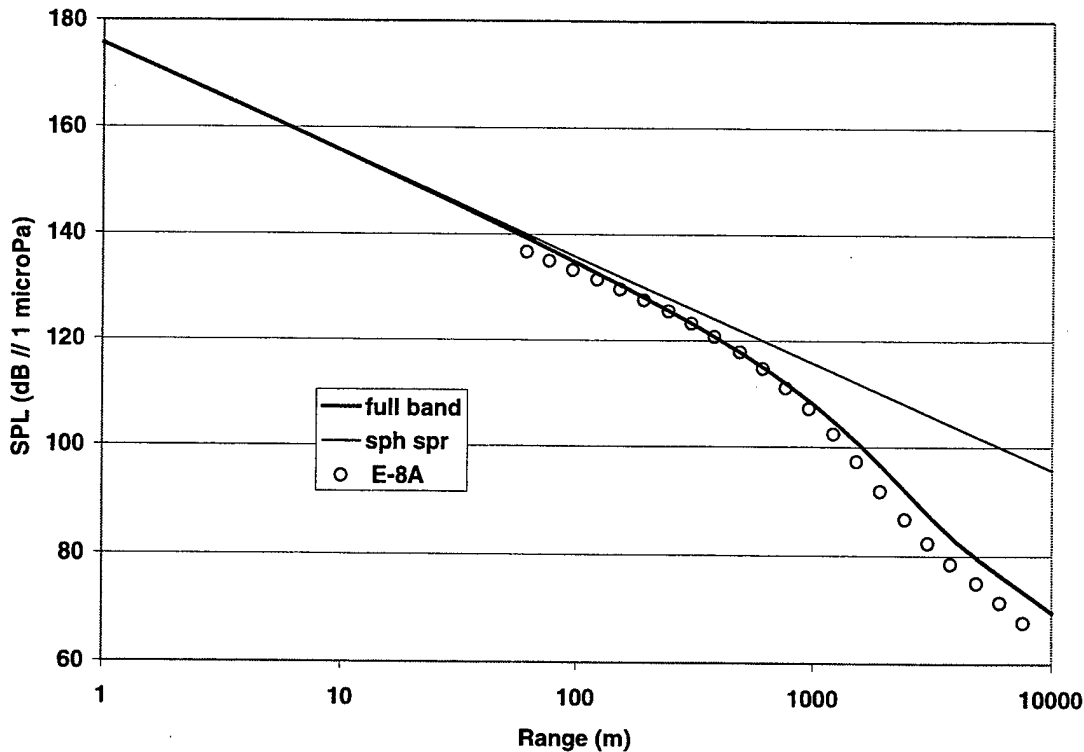
Figure 3.3-7 Full-band propagation sound pressure level for E-8A aircraft as a function of distance.

3.4 Coupling into Waterborne Long Range Propagation Paths

Observations by Urick (1972) and theoretical considerations by Chapman et. al. (1992) indicate that once the acoustic signal enters the water its lateral range will be greatly extended if it couples into low loss ducts, formed either by an upward refracting sound speed profile or by a low-loss reflecting bottom. The effects of coupling into lateral propagation paths is likely to be most pronounced in shallow water. In deep water the signals would undergo severe attenuation by spreading over the long path lengths before becoming reflected or refracted back toward the surface.

Numerical results, presented in Section 3.6.4, describe the coupling and lateral extension of the pressure field in an isovelocity shallow water channel. Typically in shallow water, long range propagation paths exist for paths with grazing angles less than some critical, which over sand bottoms can be as high as about 30 degrees. Countering the effectiveness of the coupling is the fact that the dipole character of the sound that enters the water discriminates against the low grazing angle paths.

3.4.1 Bottom reflection loss

The environmental parameter with most control over the propagation is the bottom reflection loss, which in simple cases can be quantified in terms of a plane wave reflection coefficient that

3-19

gives loss as a function of the wave grazing angle. A set of four representative loss versus angle curves for various bottom sediments is presented in Figure 3.4-1. These curves give bottom reflection loss for a bottom half space [Eller and Gershfeld, 1985], based on the bottom sediment parameters in Table 3.4-1 [Hamilton 1972, 1974]. The sediment plane wave attenuation coefficient, expressed in dB/m-Hz, is assumed to be linear in frequency for these sediments. A result of this assumption is that the loss per bounce in Figure 3.4-1, is independent of frequency. These assumptions would not hold if one were to consider bottom regions with layered or other depth dependent structure. The purpose of the present investigation, however, is to indicate a physical basis for what can happen, more than to give predictions for actual specific environments.

Table 3.4-1 Parameter values used to compute bottom reflection loss

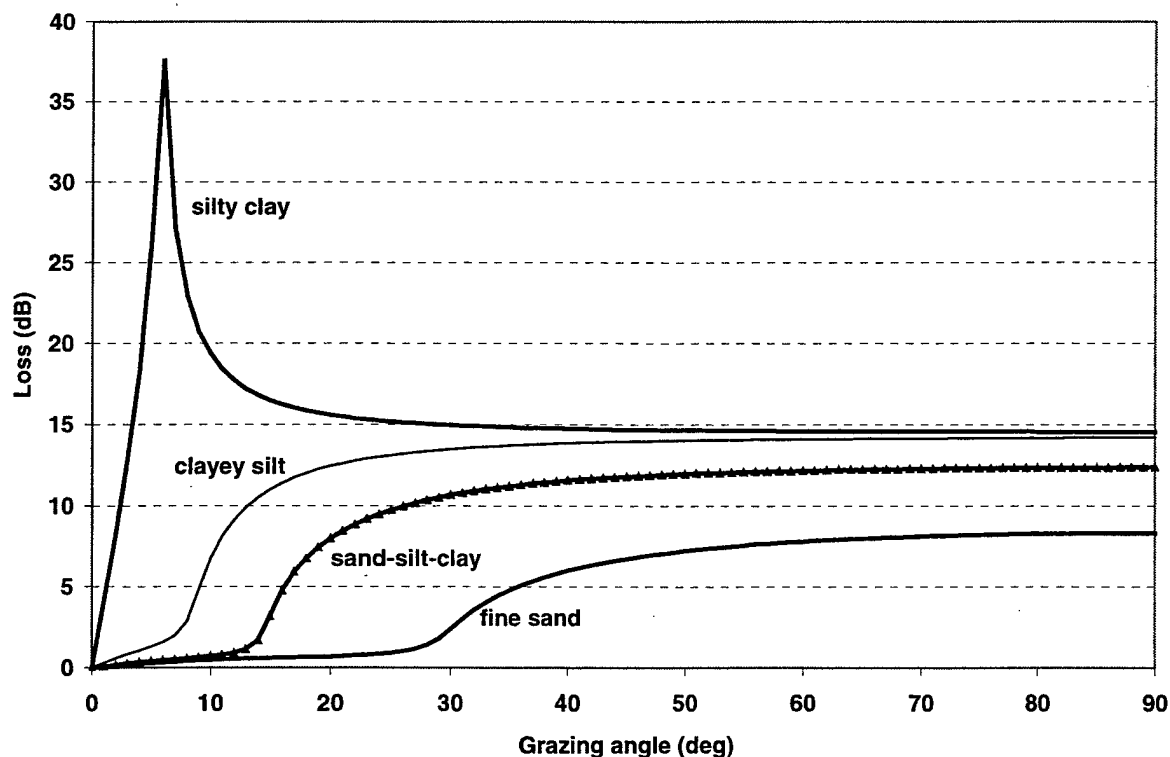| parameters	sediment			
	fine sand	sand-silt-clay	clayey silt	silty clay
sound speed ratio	1.147	1.033	1.011	0.994
density ratio	1.957	1.583	1.469	1.400
atten. coeff. dB/m-Hz	0.00051	0.00011	0.00008	0.00002

Figure 3.4-1. Plane wave bottom reflection loss curves for four bottom sediments.

3-20

3.5   Ambient Noise in the Ocean

As a lower bound on sound pressure levels experienced in the ocean, a nominal level of the ambient noise is presented here. The nominal ambient noise consists of noise from distant ships and wind related noise generated at the surface.

There are a number of well-known empirical and analytical models available (see, e.g., Urick, 1983, for Knudsen and Wenz spectra). For this report, a convenient set of formulas for the omnidirectional noise spectral density from 10 Hz to 10,000 Hz is taken from the Generic Sonar Model (GSM) documentation by Weinberg (1985).

Shipping noise level (dB) = $76 - 20 (\log(\text{freq}/30))^2$

for frequencies (freq) from 10 to 10,000 Hz,

Wind noise level (dB) = $44 + \text{sqrt}(21\ W) - 17 (\log(\text{freq}) - 3) (\log(\text{freq}) - 2)$

for frequencies from 10 to 1000 Hz,

and

Wind noise level (dB) = $95 + \text{sqrt}(21\ W) - 17 \log(\text{freq})$

for frequencies from 1000Hz to 10,000 Hz.

The total omnidirectional ambient noise spectrum level to be used in this report as a baseline reference is then given by the decibel sum, i.e.,

Reference noise level

= 10. log[10.**(shipping noise level/10) + 10.**(wind noise level/10)]

In the expression for shipping noise level, a parameter for shipping level used by Weinberg was set to a default value of 4 and does not appear above. Furthermore, *freq* indicates frequency in Hz, and *W* is wind speed in knots.

It is emphasized that this ambient noise model is used for convenience. Actual noise levels depend on propagation conditions and the details of the shipping field. As such, these reference levels could have been much greater or smaller, especially at the lower frequencies.

Table 3.5-1 presents values of noise spectrum levels at each 1/3-octave band center frequency and noise band levels in each 1/3-octave band. Levels for the total of all 24 bands and for the low frequency and high frequency bands, are given, also. Figure 3.5-1 shows the shipping and wind related noise components (for a wind speed of 15 knots), as well as the combined noise from both sources, and the band levels in the 1/3-octave bands.

Table 3.5-1 Ocean ambient noise in 1/3-octave bands

1/3-octave-band center frequency (Hz)	spectrum level at 1/3-octave-band center frequency (dB//1 microPa^2/Hz)	1/3-octave-band level (dB//1 microPa^2)
50	75.1	93.0
63	74.0	92.9
80	72.6	92.5
100	71.1	92.0
125	69.5	91.4
160	68.0	91.0
200	67.1	91.0
250	66.6	91.5
315	66.3	92.2
400	66.0	92.9
500	65.4	93.3
630	64.5	93.4
800	63.2	93.2
1000	61.8	92.7
1250	60.1	92.0
1600	58.3	91.2
2000	56.6	90.5
2500	55.0	89.9
3150	53.3	89.2
4000	51.5	88.4
5000	49.9	87.8
6300	48.2	87.1
8000	46.4	86.3
10000	44.7	85.7

total energy level = 105.2 dB for the 24 bands from 50 to 10000 Hz
total low frequency energy level = 104.2 dB for the 17 bands from 50 to 2000 Hz
total high frequency energy level = 102.2 dB for the 14 bands from 500 to 10000 Hz
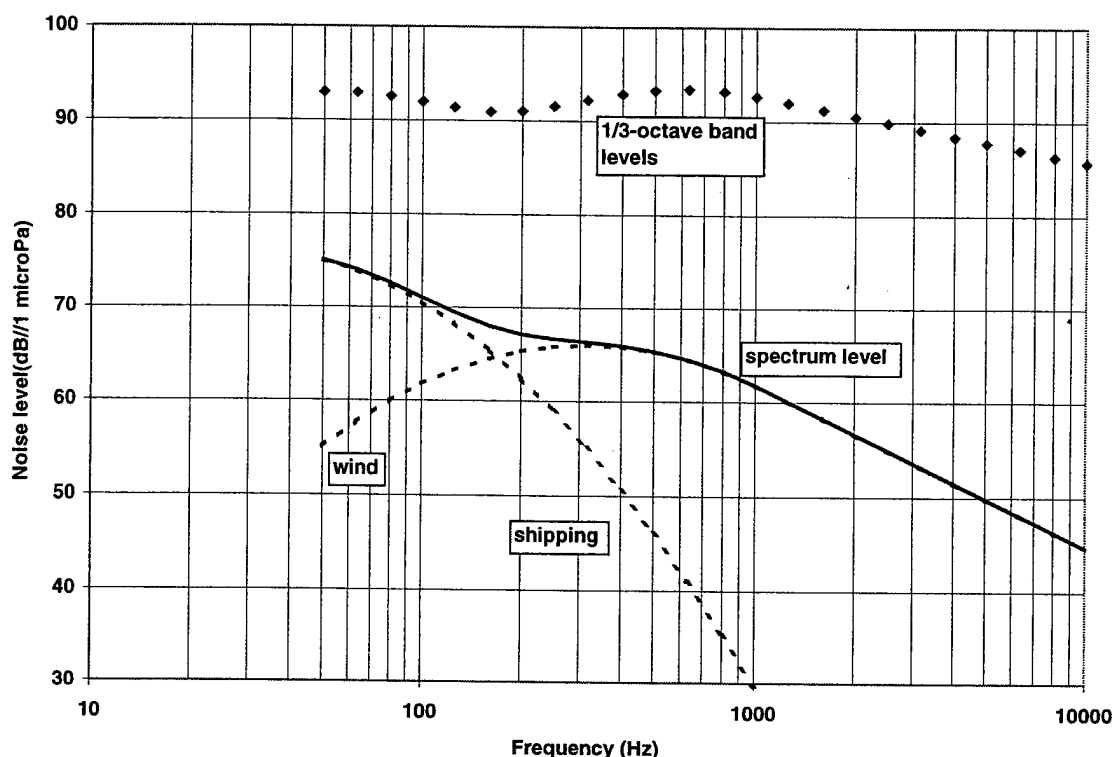
3-22

Figure 3.5-1 Representative Omnidirectional Ambient Noise Spectrum Levels for moderate shipping and a wind speed of 15 knots

3.6   Methods for Computing Noise Properties

This section presents computed results for the pressure level in the water resulting from a source in air. The computations are based on a ray theoretic analysis, the evanescent field contribution outside the critical region, and the effect of rough surface scattering. The effects of bottom reflected sound in an isovelocity shallow water channel are addressed also.

3.6.1   Computation of direct Sound Pressure Level distribution by ray theoretic results

Computed results for the distribution of pressure level in depth and horizontal direction were computed from the following set of equations based on the ray analysis as presented by Hudimac (1957) and Pierce (1981). For the purpose of presenting and comparing computed results, it is convenient to normalize the results by giving pressure amplitude relative to its value P_{10} in air at the air-water interface directly under the source. The pressure P_{10} is related to the source strength P_1 by

$$P_{10} = P_1 / h.$$

Using this and normalized range and depth variables $u = x/h$, and $v = z/h$, one may recast Eq. 6 as

$$P_2 / P_{10} = \frac{2 \cos \theta_1}{[\ 1 + v(c_2/c_1)\ (1/B)]^{1/2}\ \ [1 + v(c_2/c_1)\ (1/B^3)]^{1/2}} \qquad (13)$$

where $\qquad \theta_2 = \arcsin\ [(c_2/c_1)\ \sin\theta_1]$,

and $\qquad B = \cos \theta_2/\cos\theta_1.$

In addition, one has the geometrical relation

$$u = \tan \theta_1 + v \tan \theta_2 \qquad (14)$$

to relate lateral distance u to the angles.

The significance of this result is that in Eq. 13 all explicit dependence of the field structure on height of the source is removed. The equation gives a universal picture of the structure of the field in the water that can be scaled to apply to any value of source height.

This set of equations was solved recursively using circular cell references in an Excel spread sheet to give the pressure field P_2 as a function of normalized position coordinates u and v as independent variables. The results for an assumed level P_{10} of 100 dB are presented in Figure 3.6-1, which shows the spatial distribution of the sound field in water. This figure presents the pressure field level in relation to the pressure amplitude in air at the air-water interface. When expressed in terms of the normalized spatial coordinates, the result is a universal graph, independent of the height of the source in air. According to these results the pressure amplitude is greatest in the water right at the interface directly under the source. Sound levels are generally high in the zone directly beneath the critical region defined by the 13-degree cone.

The results of Pierce are compared to results from the simplified expressions of Young (1971,1973) and Urick (1972) in Figures 3.6-2 and 3.6-3. Values of directly transmitted SPL were predicted as a function of lateral range along a fixed depth in the water by each of the three models. Using the Pierce result as the correct result, one sees that the Young result is valid only at short range and the Urick result at long range. Possibly the only advantage to including the two approximations is ease of computation. The Young and Urick results can be computed directly to give pressure with range and depth being independent variables. The Pierce results, on the other hand, give only an implicit functional relation and cannot be solved directly to give pressure at pre-selected values of range and depth.

3.6.2 Evanescent Contribution

The evanescent pressure field amplitude resulting from a point source P_1 is computed from Eq. 3, rewritten as

$$P_2 = P_{1s} \, T \exp(- \, 2\pi \, \gamma \, z/\lambda_2) \, , \tag{15}$$

where P_{1s} is the pressure amplitude in air at a point at the water surface outside the $13°$ cone and directly above the measurement point. Computed values of the pressure level as a function of depth for the direct transmission (ray theoretic result) and the evanescent field are compared in Figures 3.6-4 and 3-6.5.

3.6.3 Effects of Rough Interface Scattering

Estimates for the effect of transmission through a rough interface were computed on the basis of Equation 16 below, using the concept underlying Equation 11, in which the grazing angle in water is replaced by an effective value that includes the slope statistics. Equation 16 is a combination of Equation 13 for the direct transmission and Equation 11 based on Lubard and Hurdle (1976). Thus, the pressure in water contributed by rough interface scattering of the direct transmission is given by

$$P_2 / P_1 = \text{[Result from Eq.(13)]} * [\sin (\phi^2 + \, <\alpha^2>)^{1/2} / \sin \phi]. \tag{16}$$

The final term represents the influence of the rough surface as a multiplicative factor, and $<\alpha^2>$ is the rms slope of the surface. Figure 3.6-4 displays a vertical slice of the pressure field near the surface and indicates the modification of the direct field because of rough interface scattering. The evanescent contribution is as before.

3.6.4 Effects of bottom reflected (ducted) sound in an isovelocity shallow water channel

Using Urick's (1972) initial observation that the source in air could be replaced by a dipole of reduced strength at the air-water interface, a simple ray trace code was written to estimate the SPL as a function of range and depth in an isovelocity shallow water channel with a lossy bottom. Use of this approximate approach is expected to be valid at slant ranges in the water substantially greater than the height of the actual source in air. The technique of replacing the source in air by an equivalent source in water is examined further by Chapman, Thompson and Ellis (1992) in order that a variety of acoustic propagation models could be applied to address arbitrary acoustic environments. The present application is restricted to the somewhat simpler case however.

In the ray trace code all ray paths are included, up to a limit of 200 bottom bounces. The loss along each path is determined by spherical spreading along the total slant range of the ray path and by the number of bottom bounces with the loss per bounce as given by the model used to

produce Figure 3.4-1. Phase was not included, and the intensities of all ray paths were added together. A directionality factor of $\cos^2\theta$ is applied to the intensity of each ray, where θ is the angle of each ray measured from the vertical.

Results of the isovelocity model for the SPL along a horizontal path at two different depths in water are presented in Figure 3.6-6 and compared to results from the Pierce, Young and Urick models. Parameters used in the calculations are

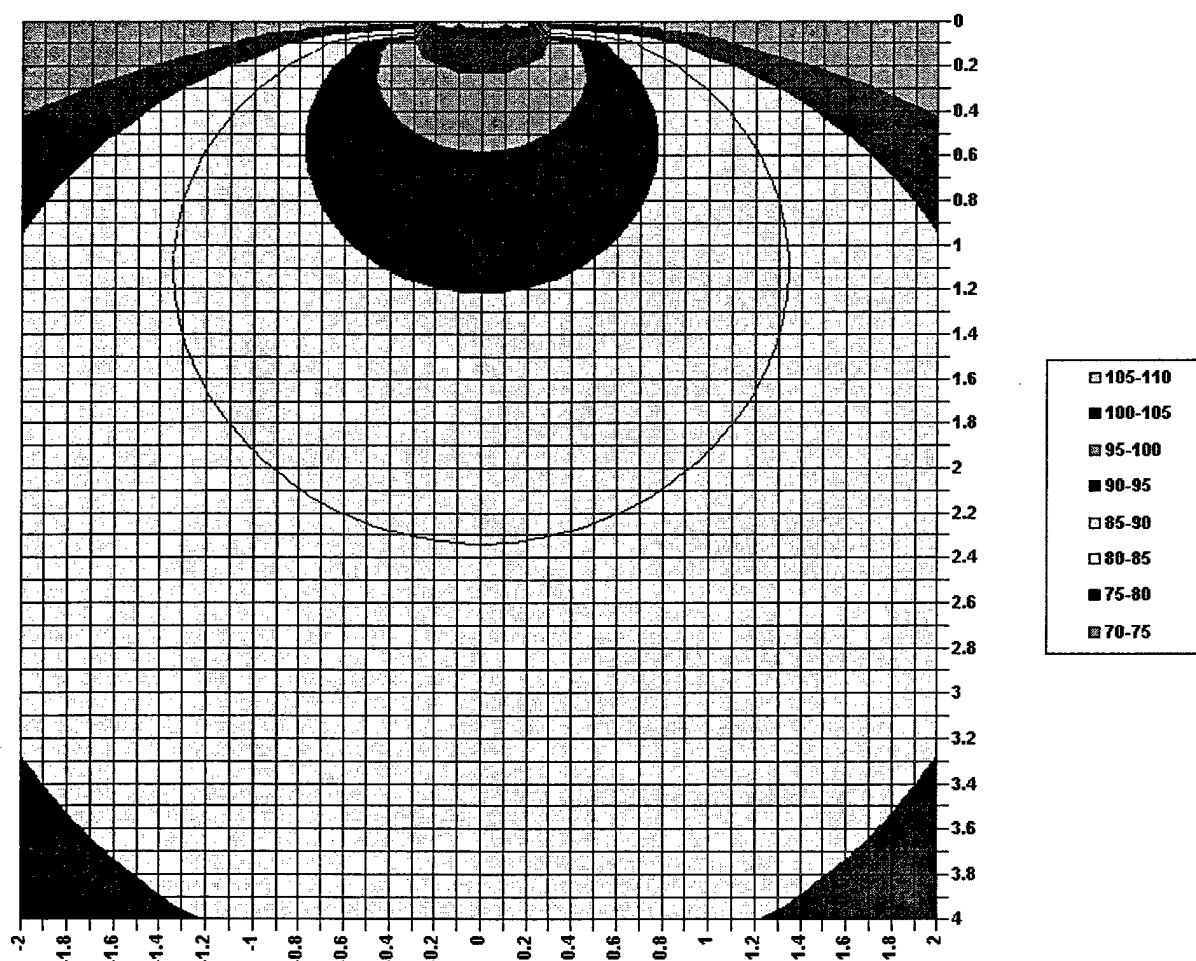| Water depth	200 m		frequency	200 Hz
altitude of source	1000 m		Source level in air	175 dB // 1µPa @ 1 m
sensor depth in water	50 m		Dipole source level in water	168 dB // 1µPa @ 1 m
sediment type	sand-silt-clay			

Figure 3.6-1. Universal depiction of the field structure in water for a field strength in air at the air-water interface of 100 dB. Depth and lateral distances are expressed as multiples of the height (altitude) of the source in air above the water.
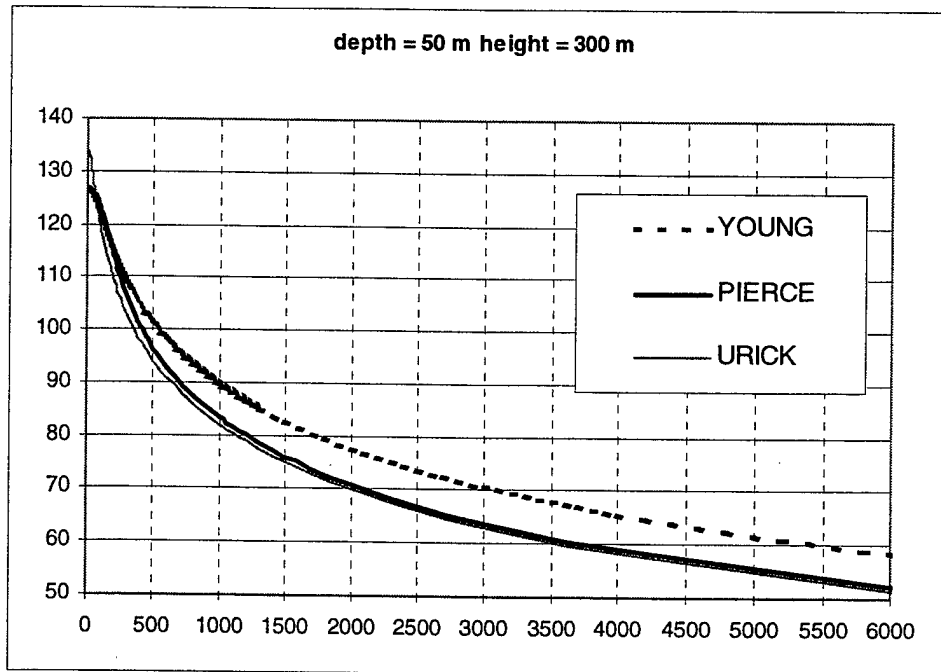
Figure 3.6-2. Comparison of three predictions of SPL as function of horizontal range at fixed depth of 50 m for a source of 175 dB at height of 300 m.
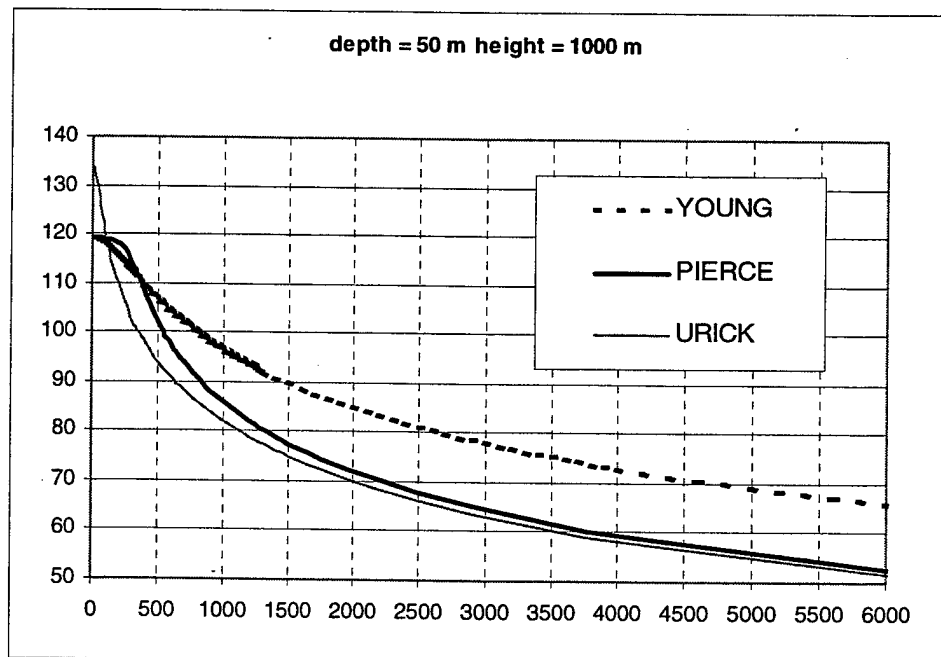

Figure 3.6-3. Comparison of three predictions of SPL as function of horizontal range at fixed depth of 50 m for a source of 175 dB at height of 1000 m.
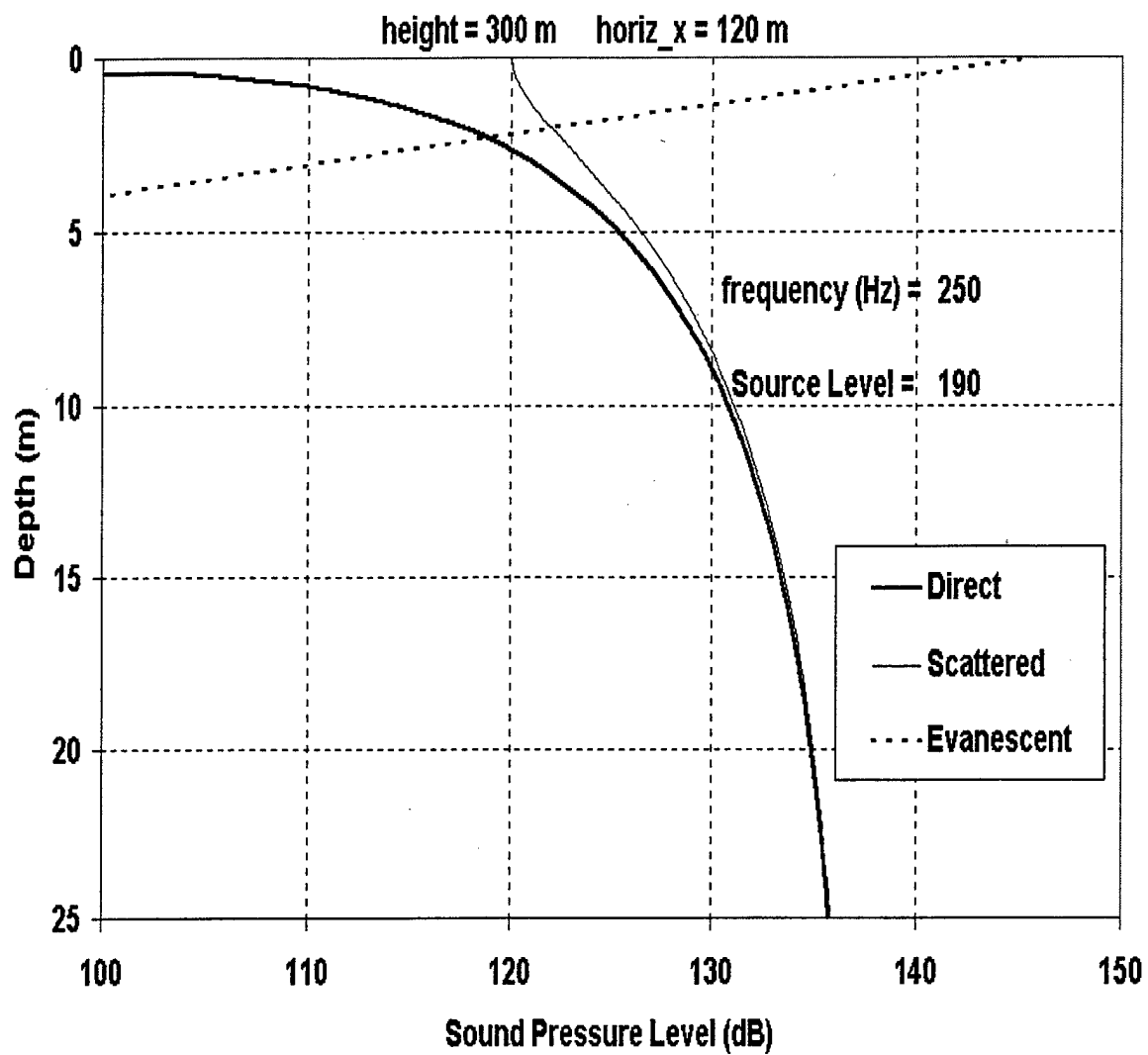
Figure 3.6-4. Vertical pressure profile at a lateral range of 120 m for direct and evanescent contributions at a frequency of 250 Hz for a 190-dB source, 300 m above the water.

depth = 2 m   height = 1000 m

source 175 dB, 80 Hz

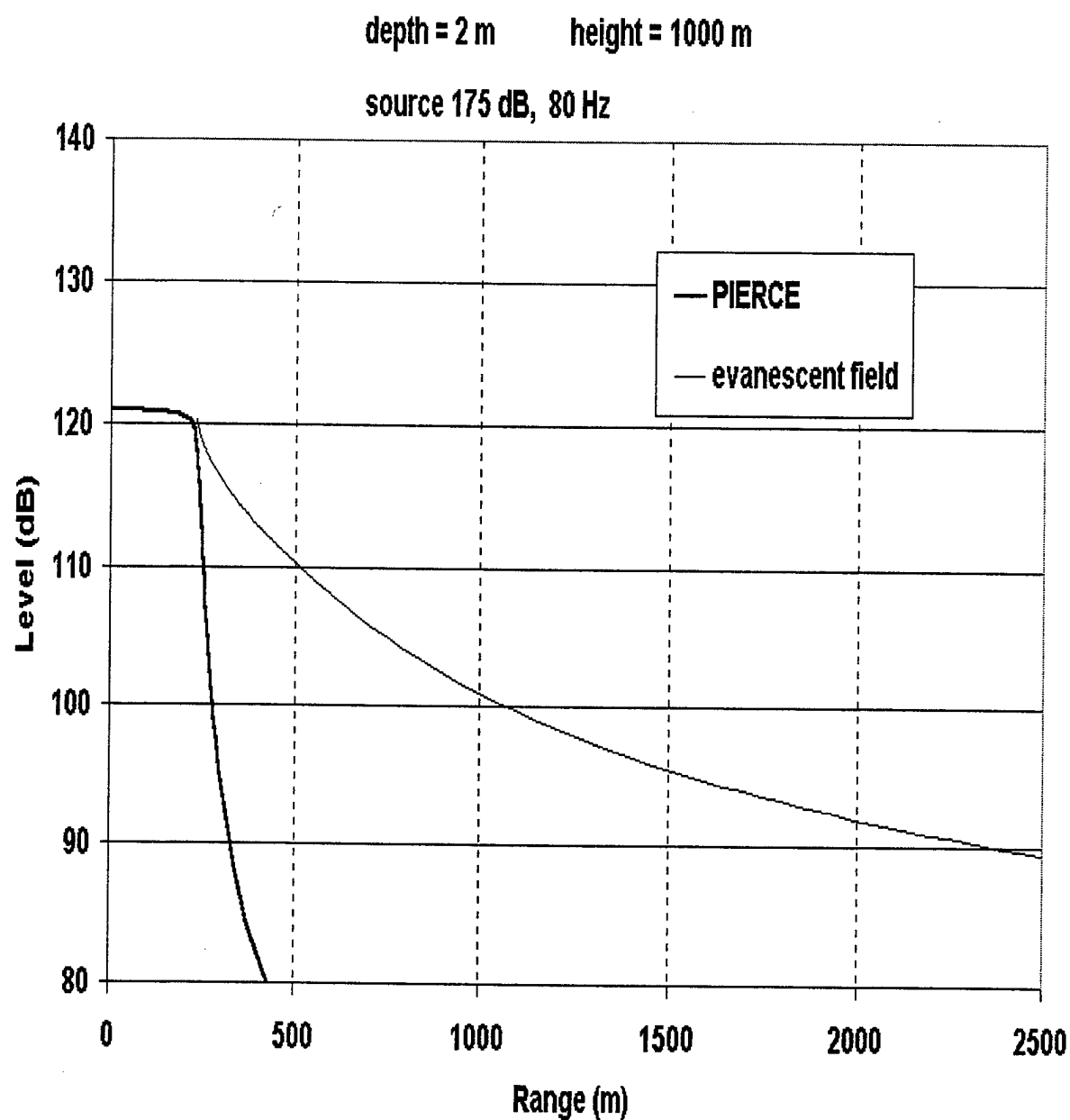Figure 3.6-5. Sound pressure level by direct and evanescent paths as a function of horizontal range at a depth 2 m beneath the water surface for a 175-dB sound source at 80 Hz, located 1000 m above the water.

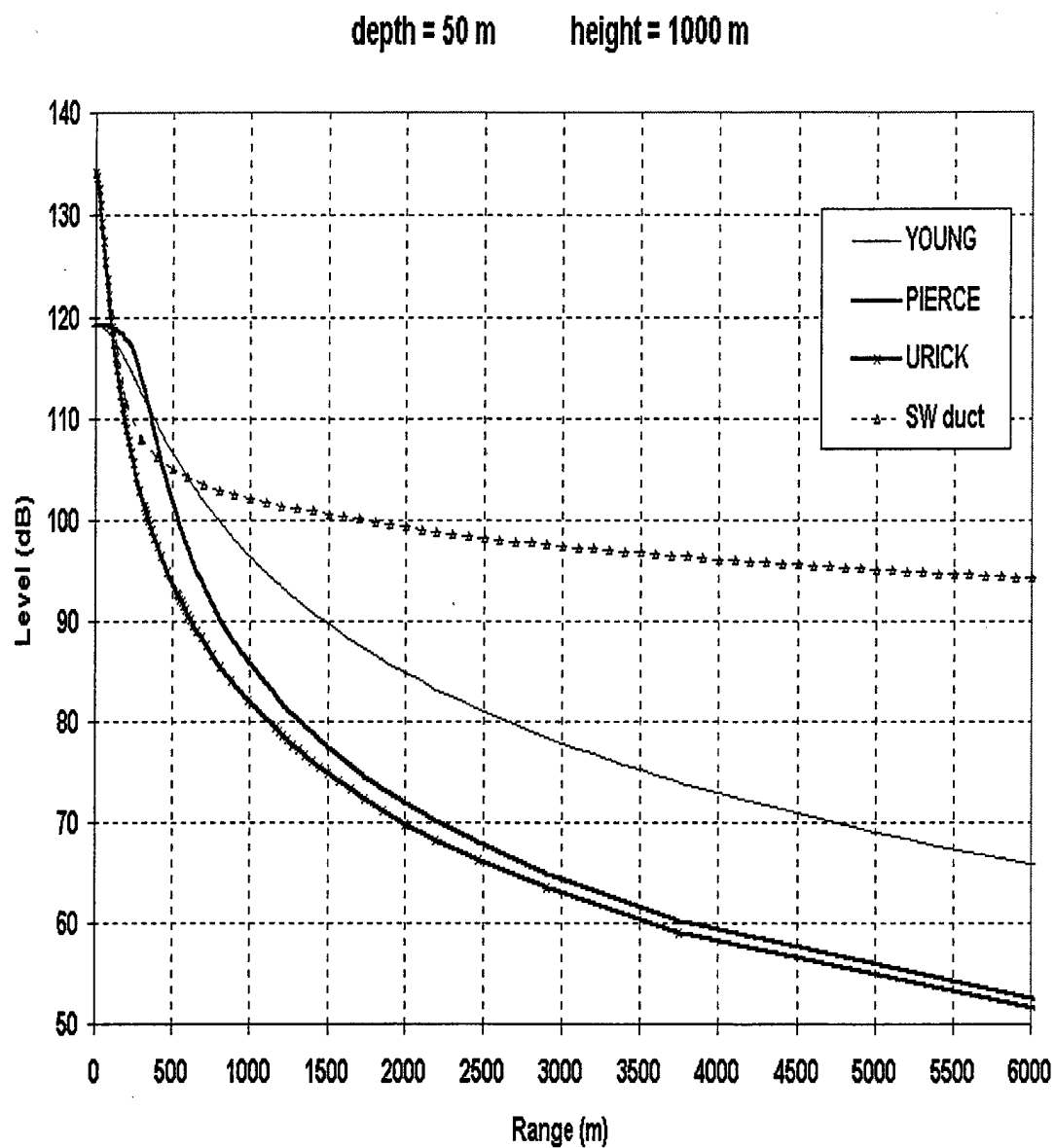depth = 50 m   height = 1000 m

Figure 3.6-6. Comparison of four predictions of SPL as function of horizontal range at fixed depth of 50 m for a source of 175 dB at height of 1000 m.

3-30

4.0 ILLUSTRATIVE EXAMPLES OF RISK ESTIMATES

This section presents estimates of sound pressure level (SPL) as a function of time at selected underwater locations as an F-18 aircraft flies overhead at various heights. Earlier calculations presented in Section 3 were intended to be illustrative of the contributing physics looked at singly and compared to each other. In the following calculations, all relevant effects are included. The overall intention of the presentation is to identify conditions under which noise levels may exceed thresholds of concern and to indicate how such results can be computed. Parameters included in the results are identified in Table 4.0-1.

Table 4.0-1. Parameters used in the Risk Estimate study

Aircraft – from data base	F-18 at 250 knots
Altitudes (heights) of aircraft above water	300 m, 1000 m, 3000 m
Depths of receiver (animal) beneath water surface	2 m, 10 m, 50 m
Frequency bands	LF: 50 – 2,000 Hz HF: 500 – 10,000 Hz
Graphical format	SPL (component parts) for selected cases vs time from -30 sec to + 30 sec
Water depths	Deep water, "infinite depth" (no ducting or bottom return); Shallow water, 200 m deep isovelocity channel, with sand-silt-clay sediment bottom

The F-18 was selected because it is one of the more noisy of Air Force aircraft.

4.1 Computation Method

The following approach was used to prepare the graphical information. The direct contribution was calculated from Eq. 13. The sound source was described in terms of the one-third octave band source levels given for the three aircraft in Table 3.3-1. Absorption losses in air were also taken into account on a frequency-by-frequency basis along with the absorption coefficients given in Table 3.3-3. Absorption loss was computed for a distance equal to the height h of the sound source above the water surface. The slight increase of the path in air for rays at the edge of the 13° cone , approximately $1.026\,h$, was not accounted for, and no account was made of the absorption losses in the water.

The influence of rough surface scattering is included by means of Eq. (16).

The evanescent contribution is computed from Eq. (15) on a frequency-by-frequency basis, in one-third-octave bands, using the aircraft source level associated with each band in Table 3.3-1. Pressure amplitude P_{1s} is determined from P_1, the amplitude at the reference distance of 1 m, by accounting for the spreading and absorption losses in air. These are computed for each frequency band using the absorption coefficients in air from Table 3.3-3 and the slant range from

4-1

the source in air to the point on the water surface immediately above the measurement point in water.

The pressure amplitudes occurring in the shallow water duct are determined by the procedure described in Section 3.6.4. All of the effects of altitude and frequency-dependent absorption are incorporated into the value of the dipole source level. Absorption loss in air is computed on a frequency band by frequency band basis using the specified source level in each band and the appropriate absorption coefficient for each band. Dipole source levels for the F-18 aircraft at the three source heights considered are presented in Table 4.1-1.

The computed results are, in essence, quasi-static functions of horizontal position and are converted to time for a source moving at 250 knots.

Table 4.1-1. Dipole source level values in dB re 1 μPa at 1 m for F-18 aircraft above water

Source Altitude (m)	Low-Frequency Band	High-Frequency Band
300	189	187
1000	188	183
3000	185	178

4.2 Discussion

Computed results, presented graphically, are collected in Appendix B. They demonstrate for the F-18 aircraft that substantial levels, that is levels in excess of 120 dB are found in water. The primary propagation and coupling effect is the direct propagation within the 13° cone and penetration into the water. This mechanism produces the largest underwater sound levels.

The evanescent field also is significant for measurement points close to the surface. The evanescent field can extend significantly the range, and hence the temporal duration, where the SPL exceeds 120 dB.

Ducted paths, such as those included in the shallow water channel figures can overshadow the direct and evanescent contributions at long range. For the figures in Appendix B that refer to shallow water, the ducted contributions, although presented at all times, are valid only outside the intense direct contribution region.

Perhaps more important is the obverse view. Namely, it is difficult to construct cases (for any aircraft at any altitude in any propagation environment) for which the underwater noise is sufficiently intense and long lasting to cause harassment or injury to any form of marine life under criteria and thresholds in common use today. In mind is the observation that in-water harassment thresholds for marine mammals and sea turtles are generally above 150 dB (re 1 μPa), except for long–term exposure (minutes to days).

It is argued here that noise in water from subsonic Air Force aircraft will almost never have impact on protected species - and that cases of concern can be identified in advance and avoided or mitigated.

5.0 GLOSSARY OF TERMS

c_1, c_2	speeds of sound in air, water, respectively	used in Eq.(1)
θ_1, θ_2	angles of incidence (measured from the vertical) in air, water, respectively	used in Eq.(1)
ρ_1, ρ_2	densities of air, water, respectively	used in Eq.(2)
P_{1pw}, P_{2pw}	amplitudes of plane waves in air, water, respectively	used in Eq.(2)
T	ratio of plane wave amplitudes P_{2pw}/P_{1pw}	used in Eq.(2)
$p_2(x,z,t)$	acoustic pressure in water as function of position and time	used in Eq.(3)
λ	wavelength of single frequency sound wave	used in Eq.(3)
ω	angular frequency of sinusoidal wave	used in Eq.(3)
g	wave attenuation factor	defined in Eq.(5)
P_1	pressure amplitude at reference distance from noise source in air	used in Eq.(6)
P_2	pressure amplitude at field point in water	used in Eq.(6)
h	height of source in air above water surface	used in Eq.(6)
d	depth of field point in water beneath water surface	used in Eq.(6)
B	ratio of cosines	defined in Eq.(7)
R	slant distance from measurement point to point where ray crosses the water surface	used in Eq.(9)
r	distance used in Young's result as defined in Figure 3.2-3a; also used as general range in air	used in Eqs.(10, 12)
ϕ	complementary angle to θ_2	used in Eq.(11)
α	angle between normal to slope of a facet on the rough sea surface and the vertical; also the sound absorption coefficient in dB/m	used in Eqs.(11, 12)
SPL	sound pressure level in dB **re** 1 μPa	used in Eq.(12)
f	frequency in Hz	used in Eq.(12)
r_1	reference distance from source, taken here as 1 m	used in Eq.(12)
W	wind speed in knots	used in Sect. 3.5
P_{10}	pressure amplitude in air at water surface directly beneath the source	used in Eq.(13)
u, v	normalized values of horizontal and vertical distance	used in Eq.(13)
P_{1s}	pressure amplitude in air at water surface outside the 13° cone and directly above the field measurement point in water	used in Eq.(15)

6.0 REFERENCES

Cavanagh, R. C., "Final Report: Criteria And Thresholds For Adverse Effects Of Underwater Noise On Marine Animals," Science Applications International Corporation, McLean, VA, May 2000 (Revised)

Cavanagh, R. C. and H. Laney, "Final Report: Background Definitions and Metrics for Sound Properties in Air and in Water Relevant to Noise Effects," Science Applications International Corporation, McLean, VA, April 2000 (Revised)

Chapman, D.M.F. and Ward P.D. (1990), "The normal-mode theory of air-to-water sound transmission in the ocean," J. Acoust. Soc. Am. **87**, 601-618

Chapman, D.M.F., D.J. Thomson and D.D. Ellis, "Modeling air-to-water sound transmission using standard numerical codes of underwater acoustics," J. Acoust. Soc. Am. **91**, 1904-1910 (1992).

Eller, A.I. and Gershfeld, D.A. (1985), "Low-Frequency Acoustic Response of Shallow Water Ducts," J. Acoust. Soc. Am. **78**, 622-632

Finneran, J. J., Schlundt, C.E, D. A. Carder, J. A. Clark, J. A. Young, and S. H. Ridgway (2000). "Auditory and behavioral responses of bottlenose dolphins (*Tursiops truncatus*) and a beluga whale, (*Delphinapterus leucas*) to impulsive sounds resembling distant signatures of underwater explosions," J. Acoust. Soc. Am. **108**, 417-431

Gerjuoy, E. (1948), "Refraction of Waves from a Point Source into a Medium of Higher Velocity," Phys. Rev. **73**, 1442-1449

Hamilton, E.L. (1972), "Compressional-Wave Attenuation in Marine Sediments," Geophysics **37**, 620-646

Hamilton, E.L. (1974), "Prediction of Deep-Sea Sediment Properties: State-of-the-Art," in *Deep-Sea Sediments, Mechanical and Physical Properties*, ed. A.L. Inderbitzen, Plenum Press

Kinsler, L.E., Frey, A.R., Coppens, A.B. and Sanders, J.V. (1982) *Fundamentals of Acoustics*, Third Edition, John Wiley & Sons, New York

Laney, H. and R. C. Cavanagh, "Final Report: Supersonic Aircraft Noise at and beneath the Ocean Surface: Estimation of Risk for Effects on Marine Mammals," Science Applications International Corporation. McLean, VA, June 2000

Lubard, S.C. and Hurdle, P.M. (1976), "Experimental investigation of acoustic transmission from air into a rough ocean," J. Acoust. Soc. Am. **60**, 1048-1052

Moore, Sue E. and Janet T. Clarke, "Summary of Marine Mammal Occurrence and Population Estimates in U.S. Coastal Waters Subject to Military Aircraft Overflights," Science Applications International Corporation, San Diego, CA, October 1998

NOAA/NMFS (1998). "Acoustic Criteria Workshop," Sponsored by National Marine Fisheries Service (NMFS), Office of Protected Resources, Held at 1301 East-West Highway, Silver Spring, MD, 9-11 September, 1998

Pierce, Allan D. (1981), *ACOUSTICS: An Introduction to Its Physical Principles and Applications*, McGraw-Hill Book Company, New York, pp. 411-13.

Standard Eiger (1995). "Environmental Assessment of the Use of Underwater Acoustic and Explosive Sources during Exercise Standard EIGER," prepared for the Submarine Security Program Office (CNO, N875) by SAIC, July 1995 (Secret)

Stratton, J.A (1941), *Electromagnetic Theory*, McGraw-Hill Book Co., New York

SURTASS-LFA DEIS (1999). Department of the Navy, "Draft Overseas Environmental Impact Statement/Environmental Impact Statement, Surveillance Towed Array Sensor System (SURTASS) Low Frequency Active (LFA) Sonar," May 1999

Urick, R.J. (1967), *Principles of Underwater Sound for Engineers*, McGraw-Hill Book Co., New York

Urick, R.J. (1972), Noise Signature of an Aircraft in Level Flight over a Hydrophone in the Sea, J. Acoust. Soc. Am. 52, 993-999

Weinberg, H. (1985), "Generic Sonar Model," NUSC Technical Document 5971D, 6 June 1985.

Young, R.W. (1971), "Sound pressure in water from a source in air," J. Acoust. Soc. Am. **50**, 1392-1393(L)

Young, R.W. (1973), "Sound pressure in water from a source in air and vice versa," J. Acoust. Soc. Am. **53**, 1708-1716

APPENDIX A. ANNOTATED BIBLIOGRAPHY

CONTENTS

A.1 Notation

Appendix A presents a running commentary of reference texts and articles that define the state of knowledge of the transmission of sound into water from a point source in air. These articles form the basis of summarizing remarks made in the main body of the report. An attempt is made here to present all results in terms of a common notation as in Figure A1. Accordingly, results presented from these articles have their notation changed to conform to the common definition.
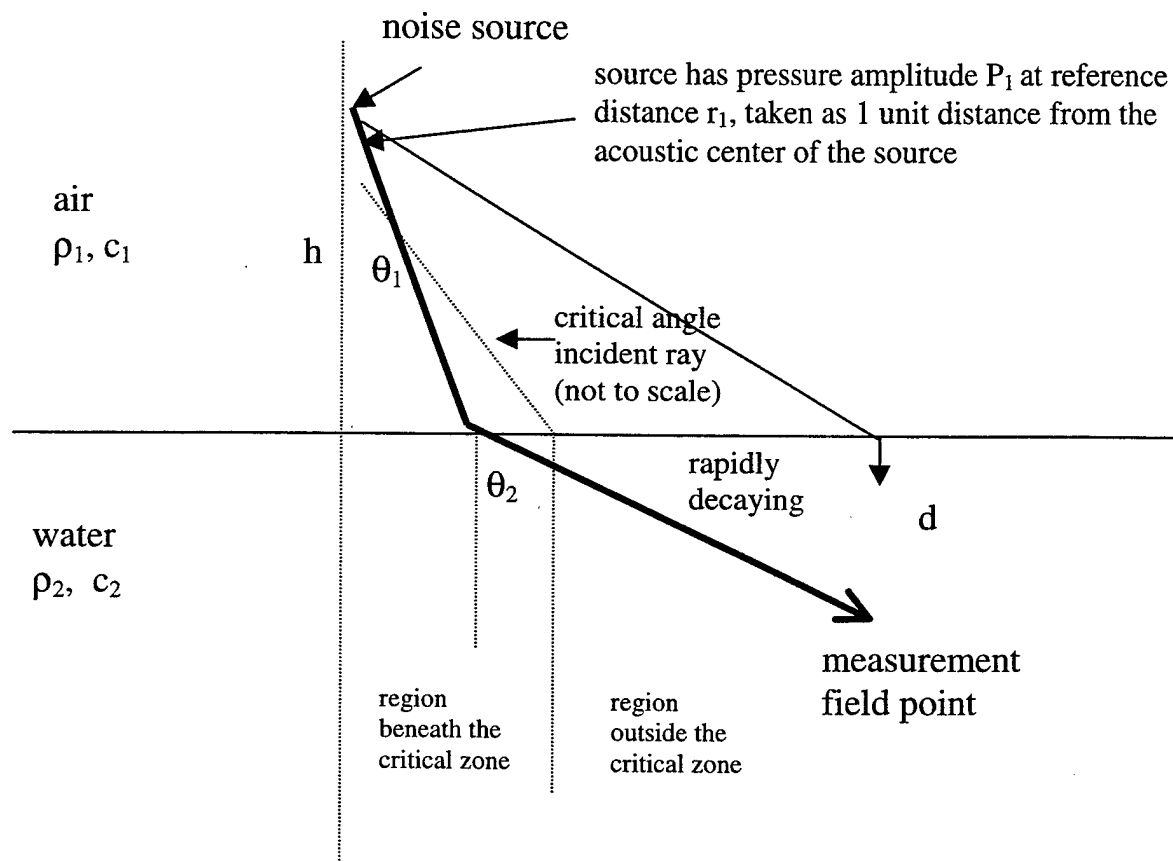

Figure A1. Geometry of the problem.

A.2 Texts

Acoustics: An Introduction to Its Physical Principles and Applications, Allan D. Pierce, McGraw-Hill Book Company, New York, 1981, pp. 411-13.

This section of Pierce's text presents a clear derivation of the ray theoretic result for the direct transmission from a point source in air to a point in the water below. Pierce's result is consistent with the result by Gerjuoy and somewhat easier to follow. The key point here is the derivation of the effect of the interface on the ray divergence. Pierce's result (his Eq. 8-7.7) is rewritten below, with consistent notation, using the value 2 in place of the full expression for the plane wave pressure transmission ratio and assuming a single-frequency sinusoidal signal:

$$P_2 / P_1 = \frac{2 \cos \theta_1}{[h + d(c_2/c_1)(1/B)]^{1/2} \; [h + d(c_2/c_1)(1/B^3)]^{1/2}}$$

where $B = \cos \theta_2 / \cos \theta_1$.

Pierce does not address the evanescent field.

Introduction to the Theory of Sound Transmission, C. B. Officer, McGraw-Hill Book Company, New York, 1958, Boundary Conditions pp 74-82, Reflectivity pp. 185-198.

The first passage cited presents an authoritative derivation of the reflection and transmission coefficients for a plane wave incident on a planar interface. Note that his results refer to the velocity potential and will differ by a factor ρ_1 or ρ_2 from the corresponding results presented in this review. Officer includes a discussion of the case of total reflection and the associated evanescent wave field. "There is no transmission of energy into the lower medium, and the amplitude decreases exponentially away from the surface into the lower medium. This wave is in no sense a free wave; it can exist only as a consequence of reflection at angles of incidence more grazing than critical and is constrained to move along the boundary with the trace velocity of the reflection along the boundary. It is a diffraction effect across the interface associated with and bound to the reflected wave."

The second passage cited presents a formal mathematical solution for the point source in the vicinity of a plane boundary. Officer concentrates primarily on the reflection term, rather than the transmission term. The integrals involved are evaluated for high frequencies by the method of stationary phase, and Officer concludes that the approximations used are valid for high frequencies and for moderate distances away from the source, and that it breaks down completely for incidence angles near critical.

Following a different approach for the case in which the lower medium is faster than the upper medium, Officer identifies three arrivals in the upper medium at large horizontal distance from the source. These are (1) a direct air-borne arrival, (2) the customary reflection arrival at angles

above critical, and (3) what Officer calls a refraction arrival. The refraction arrival enters the water at the critical angle, propagates horizontally parallel to the surface at the sound speed, and finally re-enters the water at the critical angle. The signal amplitude received in air is given by Officer's equation (5-66) on p. 195. Officer has this to say about the refracted arrival: "The ray path is a true Snell's law minimum time path. From ray acoustics alone, however, no energy would be associated with this path; from the more formal solution we see that this is not the case."

***Fundamentals of Ocean Acoustics,* L. Brekhovskikh and Yu. Lysanov, Springer-Verlag, New York, 1982, Reflected Wave pp. 76-81, Lateral Wave pp. 81-84.**

This text addresses the full solution of the problem of a point source above a boundary between two fluids. Emphasis is on the reflection in the upper medium. For large distances from the source, measured in wavelengths, a solution is found by the method of stationary phase. The authors also look at the next order of correction to the solution and show that it vanishes at high frequency with the result that the customary ray solution is valid at high frequency, with the plane wave reflection coefficient appropriate for the incidence angle. They also indicate that the geometrical acoustics solution breaks down when either the source or receiver is too close to the interface or when the incidence angle approached the critical angle.

For incidence at the critical angle, a transmitted wave is generated parallel to the interface in the water. This wave then re-enters the upper medium at the critical angle. This wave, called a lateral wave by the authors, is the same as Officer's refraction arrival.

***Waves in Layered Media*, L. Brekhovskikh, Academic Press, New York, 1960,**

The Reflection of a Plane Sound Wave at an Interface Separating Liquid and Gaseous Media pp. 15-22. Brekhovskikh presents the standard results, following closely the presentation of Officer, including the case of total reflection at angles above critical, and the associated exponentially decreasing wave in the lower medium. The exponential decay is described by his equation (3.27) as $\exp(-\delta D)$ where D is the depth and $\delta = k \operatorname{sqrt}(\sin^2\theta - (c_1/c_2)^2)$. The decay rate is seen to be a function of incidence angle.

The Reflection of a Spherical Wave at a Plane Interface – Lateral Waves pp. 270-280. Brekhovskikh describes how to treat the integration path for the case when the incidence angle exceeds the critical angle. The lateral wave, as described by Brekhovskikh, consists of two segments in air that propagate at the critical angle toward and from the surface, and a middle segment that propagates along the water interface at the speed of sound in water. The term lateral wave is used to indicate the air arrival that is shed from the water-borne propagation path parallel to, and beneath, the surface. This water-borne path is the continuous result when the direct transmission field approaches the case of critical incidence angle. Brekhovskikh interprets the lateral wave in connection with his Figure 98 on p.275.

"At the point B, sufficiently far from the source O, but situated near the boundary in the lower medium, the wave is incident along the two paths corresponding to the rays OAB and OC. The ray OC is incident on the boundary at an angle greater than the angle of total internal reflection, and being totally reflected, creates a wave in the lower medium which is attenuated exponentially with depth. The ray OA undergoes the usual refraction, and travels along AB in the lower medium to the point B. The closer the ray OA approaches the dotted line OD, corresponding to the angle of total internal reflection, the closer will the ray AB approach the boundary. The wave represented by the ray AB is the cause of the lateral wave. In fact, it propagates along the boundary with the velocity [of sound in water], creating a corresponding disturbance on the boundary. This gives rise to a new wave in the upper medium. ...

"As an additional basis for the above considerations, it can be shown ...that the entire wave process propagating along the boundary can be separated into two groups of waves. The first group contains the usual incident wave (ray OC, Fig. 98), the corresponding reflected wave, and the exponentially attenuating refracted wave CB. The second group contains the wave travelling along the path OAB, and the lateral wave. Each group propagates along the boundary with its own velocity, and satisfies the boundary conditions separately."

A.3 Classic paper of E. Gerjuoy

"Refraction of Waves from a Point Source into a Medium of Higher Velocity," Phys. Rev. 73, 1442-1449 (1948).

Gerjuoy presents a detailed accounting of the acoustic field entering water from a point sound source in air. The problem is simplified to its essential core by the elimination of absorption in the water. This is perhaps the earliest scientific treatment of this particular problem available in the English language and is a good example of how even this simplified problem can be a mathematical challenge at an advanced level. Gerjuoy relates this problem to the equivalent electromagnetic problem of a dipole source above the earth, examined first by Sommerfeld and later by Weyl, and summarized in the text by Stratton. [**J.A. Stratton, *Electromagnetic Theory* (McGraw-Hill Book Company, Inc., New York, 1941), pp. 573 ff.**]

Gerjuoy examines in detail the contour integration for providing a wave solution to the problem and compares explicit wave-based results to corresponding results based on ray theory. Both sets of results agree in a high frequency limit. Gerjuoy interprets the results in the following way. For the present application of a source in air over water, all points in the water receive a directly transmitted signal that strikes the interface at an angle of incidence in air less than or equal to a critical angle of about 13 degrees. The direct pressure level in the water can be computed either by Gerjuoy's equation 32, based on an asymptotic expansion of wave theory, or his equivalent equation 40, based on ray theory. Furthermore, points in the water that lie below regions on the surface outside the critical angle also receive an exponentially decaying term,

which is given by his equation 33. At field points near the surface and sufficiently outside the critical angle, the exponentially decaying term is greater than the directly transmitted pressure.

A.4 Ray Theoretic Results

"Ray Theory Solution for the Sound Intensity in Water Due to a Point Source above It," A. A. Hudimac, J. Acoust. Soc. Am. 29, 916-17 (1957)

Hudimac presents a ray theory result for the pressure in the water consistent with, and apparently independent of, the corresponding result by Gerjuoy. He notes that the theory will break down at long range near the surface and should be replaced by a wave theory.

A.5 Wave Theoretic Results

"Wave Solution for Air-to-Water Sound Transmission," M. S. Weinstein and A. G. Henney, J. Acoust. Soc. Am. 37, 899-901 (1965)

Weinstein provides numerical integration results of the general theory of a pressure in water from a single frequency source in air. For his initial results, which address the simple problem of a water half space, the velocity potential is presented graphically as a function of field point in the water, for two heights of source above the water and for five frequencies plus a high-frequency (ray theory) limit. He states, "... the ray-theory error is not particularly large and is of importance only at low frequencies, low source altitudes, and shallow water depth. For nonzero frequencies, the curves approach the ray solution with increasing depth. The transition between wave and ray prediction occurs for $h \sim \lambda$ ...."

These results apply only to the case of a sound source directly overhead.

A.6 Results of R.W. Young

"Sound Pressure in Water from Source in Air," R.W. Young, J. Acoust. Soc. Am. 50, 1392-1393(L) (1971)

Young identifies an apparent discrepancy whereby the pressure amplitude P_2 at a depth d in the water, directly beneath a source at height h in air, is given by the low-frequency limit of wave theory as

$$P_2/P_1 = 2\ r_1/(h+d)$$

and by ray theory as

$$P_2/P_1 = 2\ r_1/(h+c_2d/c_1) = 2\ r_1\ (c_1/c_2)/(c_1h/c_2 + d)$$

where P_1 is the reference pressure at range r_1 from the source in air. Both results indicate the doubling of the pressure amplitude at the air-water boundary. Furthermore, the ray theoretic result indicates a virtual source level reduced by the factor (c_1/c_2) and a more rapid geometric spreading in the water, consistent with spreading "from a virtual source situated above the water surface approximately a quarter of the height of the actual source."

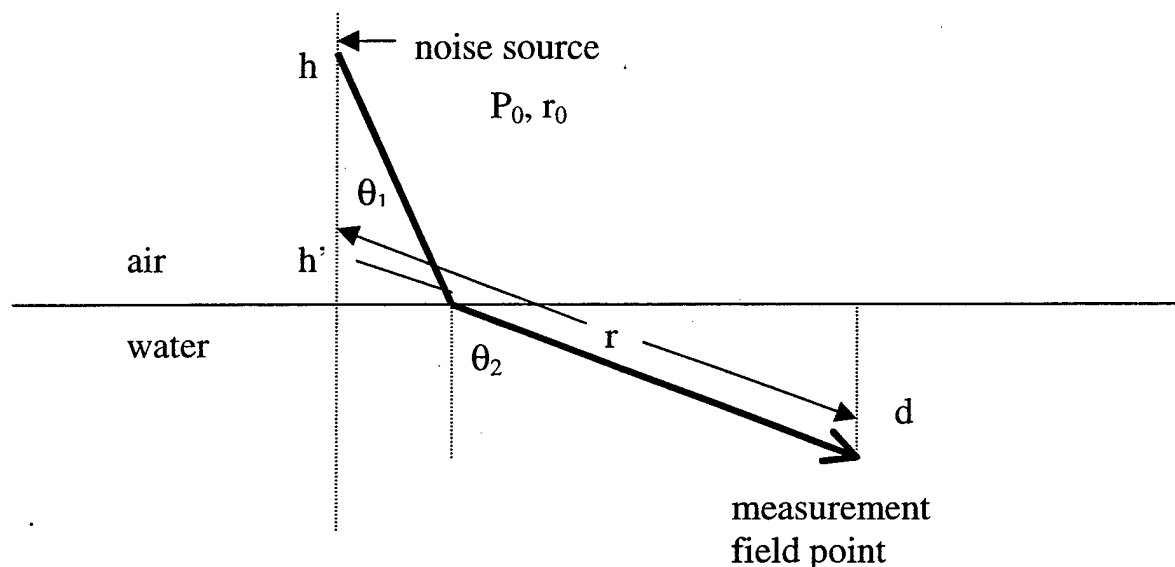Young presents measured results that confirm the ray predictions.

Figure A2. Geometry used by Young. The effective dipole source is placed at height h'.

"Comments on 'Sound pressure in water from source in air'," M.S. Weinstein, J. Acoust. Soc. Am. 53, 1756(L) (1973)

Weinstein indicates that wave theory and ray theory are in agreement when not in the low frequency limit and that Young's measurements were at sufficiently high frequency that agreement with ray theory, and associated disagreement with the low-frequency wave limit, are to be expected.

"Sound pressure in water from a source in air and vice versa," R.W. Young, 53, 1708-1716 (1973)

Young presents a simplified approach to ray calculations to determine the pressure in water from a sound source in air above the water. These calculations determine the sound level "not only directly under the source but at laterally displaced locations as well." Pressures in water are computed as though radiating from a virtual source of strength

$P_1(2c_1/c_2) \cos \theta_2$, located at height $h' = (c_1/c_2) h$,

where P_1 is the pressure at a reference distance from the actual source in air and θ_2 is the angle of the ray from the virtual source location, measured from vertical. The pressure in water is then given by

$$P_2 = [P_1(2c_1/c_2) \cos \theta_2] \, r_1/r ,$$

where r is the distance from the effective source location to the measurement field point as indicated in Figure A2.

A.7 Results by R. J. Urick

"Noise Signature of an Aircraft in Level Flight over a Hydrophone in the Sea," R.J. Urick, J. Acoust. Soc. Am. 52, 993-999 (1972)

This paper presents some summarizing remarks regarding theoretical results from the literature and some general observations of time signatures from aircraft flyovers. He reviews other contributions to ray theory but presents results only for the limiting cases of sound directly overhead, in which case he repeats the result of Young, rewritten to agree with present notation as

$$P_2 /P_1 = 2 (c_1/c_2)/ (d + (c_1/c_2)h),$$

And a far field result at slant distances appreciably greater than the height of the source, rewritten to agree with present notation as

$$P_2 /P_1 = 2 (c_1/c_2) \cos \theta_2/ R.$$

In Urick's words we can replace the real source by a dipole source located at the sea surface and radiating like $\cos \theta_2$ (in pressure), with a source pressure $2 c_1/c_2$ times that of the real source.

Data from deep and shallow water clearly show that bottom reflections in shallow water can extend the received pressure envelope in time.

Urick also presents calculations that indicate that the intensity of the evanescent field at great lateral distances and within a wavelength of the surface can be many times that of the directly transmitted field. In making this comparison Urick uses for the evanescent pressure at great lateral distance the expression, written to agree with present notation

$$P_{evanescent} = (2 P_1 /R) \exp(-kd),$$

where k is $2\pi/\lambda$.

This expression is in error because it lacks the term γ in the exponent, as shown in the discussion of the evanescent field according to Officer.

A.8 Evanescent field

"Lateral wave contribution to the underwater signature of an aircraft," J.V. McNicholas, J. Acoust. Soc. Am. 53, 1755(L) (1973)

"Comment on 'Lateral wave contribution to the underwater signature of an aircraft' [J.V. McNicholas, J. Acoust. Soc. Am. 53, 1755 (1973)]," J. Acoust. Soc. Am. 53, 1756(L) (1973)

McNicholas modifies Urick's equipressure contours by computing the coherent sum of the direct transmitted field with the evanescent field. Urick responds by pointing out that McNicholas's results are merely a modified presentation and do not contain any new material of substance not implicit in Urick's original article.

A.9 Effects of Rough Surface

"High-frequency model for sound transmission from an airborne source into the ocean," W.C. Meecham, J. Acoust. Soc. Am. 60, 339-342 (1976).

Meecham, appealing to a high-frequency limit, computes the total intensity of the received sound as the sum of the individual intensities transmitted through a statistical distribution of facets, or highlights, each oriented so that the Snell angle of the refracted ray is directed toward the receiver. His theoretical results are tailored to apply to the case of small depression angles ϕ, represented by regions near the surface and horizontally distant from the source. The approach addresses only directly transmitted paths originating with incidence angles in air within the critical angle and does not apply the scattering of the evanescent contribution. He finds, essentially, for the transmitted pressure at a submerged point near the surface and at great distance from the source, that "the intensity is the same as that for a plane ocean surface ... but modified for smaller grazing angles by $<\alpha^2>^{1/2}$ ", where α is the angle of the normal to a facet with the vertical axis. The angle indicated by $<\alpha^2>^{1/2}$ represents a floor value so that the transmitted pressure will not approach 0 at the surface. A representative value for $<\alpha^2>^{1/2}$, cited by Meecham, is 3 degrees.

It should be noted that this theory applies specifically in that region where the evanescent contribution is expected to be significant. Thus, two questions remain: How does the rough boundary contribution compare to the evanescent contribution, and does the rough boundary produce any significant alteration of the evanescent field, produced by incidence angles outside of the critical region.

"Experimental investigation of acoustic transmission from air into a rough ocean," S.C. Lubard and P.M. Hurdle, J. Acoust. Soc. Am. 60, 1048-1052 (1976).

In the form of an introduction, Lubard and Hurdle present the following general result for the pressure field in water resulting from a source in air above a smooth ocean surface.

$$P_2/P_1 = (2\ c_1/c_2 \sin \phi)\ /\ R,$$

with symbols defined as in Figure A3. This is essentially the Young result. Note that the grazing or depression angle is used here in place of the incidence angle, and distance R is measured along only the water portion of the path.

In the experiments short sinusoidal bursts were transmitted by a directional projector whose major axis was directed downward, perpendicular to the ocean surface, and received at a vertical string of hydrophones at some horizontal distance from the source. Frequencies ranged from 500 to 4000 Hz, and the geometry covers grazing angles ϕ ranging from about 3.5 to 20 degrees. The published paper refers to a vertical array, but the ensuing description suggests that individual hydrophones are used and that they are not used as an array in the sense that no beamforming is conducted.

Results are compared to the theoretical result by Meecham and Sanborn, written by Lubard and Hurdle in a form equivalent to

$$P_2/P_1 = (2\ c_1/c_2)\ (1/R)\ (\phi^2 + <\alpha^2>)^{1/2}.$$

They conclude that "[f]or the frequency range 500-4000 Hz and ocean rms slope range $1°-5°$ the data show more transmission for the rough ocean than predicted for a smooth surface, with the excess increasing at the shallower depression angles" and the "parameter $(\phi^2 + <\alpha^2>)^{1/2}$ behaves as an effective depression angle".
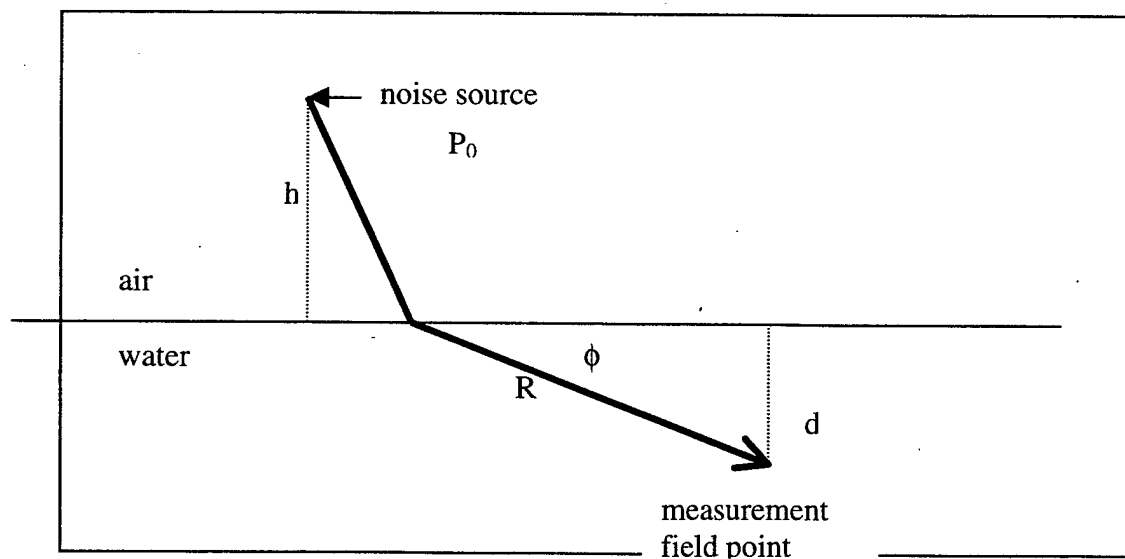

Figure A3. Geometry used by Lubard and Hurdle.

"Helmholtz-Kirchhoff Theory for Sound Transmission through a Statistically Rough Plane Interface between Dissimilar Fluids," H. Medwin and J.D. Hagy, Jr., J. Acoust. Soc. Am. 51, 1083-1090 (1972).

"Spectral characteristics of sound transmission through the rough sea surface," H Medwin, R.A. Helbig, and J.D. Hagy, Jr., J. Acoust. Soc. Am. 54, 99-109 (1973).

These first of two papers addresses the transmission of sound through a rough interface in the Kirchhoff approximation, which consists of approximating the sound field and its derivative at the interface by the values that would exist on a tangent plane at that point. These values are used to evaluate the Helmholtz integral over the interface. The paper presents and summarizes results for five cases: (1) transmission of infinite plane waves through a smooth interface, (2) transmission of aperture-limited plane waves through a smooth interface and (3) through a randomly rough interface, (4) and transmission of the field from a point source through a smooth interface and (5) through a randomly rough interface. This first paper is used primarily to establish the equations that will be used in the second paper for comparison to data. Highlights of the results are the following:

For a point source above a smooth surface, the pressure in the underlying water is given by Medwin and Hagy as (taken from their Figure 2)

$$P_2 / P_{10} = \frac{2 \cos \theta_2}{[1 + (d/h)(c_2/c_1)(1/B)]}$$

where $B = \cos \theta_2 / \cos \theta_1$, and P_{10} represents the pressure amplitude at the air-water interface directly beneath the source. Converting this to an expression for P_2 / P_1, one finds

$$P_2 / P_1 = \frac{2 \cos \theta_2}{h[1 + (d/h)(c_2/c_1)(1/B)]} ,$$

which differs from the corresponding expression from Pierce. (The equation in their Figure 2 is used as the starting point rather than their Equation 14 because there appears to be an inconsistency in converting from one to the other regarding the $\cos \theta_1$ term).

To address the problem of transmission through the rough interface, the ensonified area is divided into subareas, and then all the coherent contributions and, separately, all the incoherent contributions, are added. The results received pressure-squared are presented as the sum of a coherent and an incoherent contribution, both expressed in terms of a roughness parameter for transmission, given as

$$R = k_2^2 \sigma^2 ((c_2/c_1) \cos \theta_1 - \cos \theta_2)^2.$$

For low roughness (R<1) the transmitted mean-square pressure is coherent and is exp(-R) times the corresponding term for a smooth interface. For large roughness (R>1) the incoherent component dominates and the transmitted pressure depends also on the surface correlation length of the surface displacements.

Some issues:
The theory presented does not address the evanescent field contribution, although passing reference is made to its existence in the second paper.

The theoretical calculations are to be done by dividing the surface into a set of subareas. How to identify the appropriate subareas is not fully defined, and the computed results were found to have a weak dependence on the selection.

Values of SPL taken at submerged points directly beneath the sound source in air show substantially no dependence on roughness and exceed predictions at large roughness by more than 5 dB. In particular the data do not confirm the predicted decrease in sound level caused by the roughness. Data taken at a laterally removed point are partly in agreement with predictions in that both prediction and measurement indicate an increase in sound level with increasing roughness. Also of interest is that the predictions at low roughness show a partial shadow region near the surface and far from the source. This shadow region is filled in at large roughness by the scattered field. The measured data fill in this shadow even at low roughness and, thus, are consistent with the presence of an evanescent contribution.

The results can be summarized by the statement that the most significant effect of scattering noted through a synthesis of theoretical and measured values is the filling in of the shadow region close to the surface and far from the source.

"Transmission of sound through the scaled ocean surface," J.E. Barger and D. Sachs, Bolt, Beranek and Newman, Inc. Report No. 3103, August 1975

The authors describe the results of scaled experiments performed in a laboratory tank. Their results apply to full scale parameters, converted from the laboratory values, corresponding to frequencies from 30 to 1000 Hz, receiver grazing angles of 1 to 90 degrees, and source heights in air from 50 to 1200 ft. The sound pressure amplitude transmitted through the rough surface is a stochastic function, and their primary measurements are of (1) the mean pressure amplitude of the transmitted field for a wide set of experimental parameters and (2) the amplitude density function of narrowband pressure components for a few sets of parameters. Their results are reported in terms of the transmission gain, defined as the difference between the average band level transmitted through a rough surface and the corresponding measurement for a smooth surface.

Their basic findings are that

- Transmission gain is 0 (within 1 dB) at frequencies below 150 Hz for all sea conditions where rms heights are below SS6, for all receiver grazing angles.

- Transmission gain is 0 (within 1 dB) at frequencies below 1000 Hz for all sea conditions with rms slopes below 3 degrees, for all receiver grazing angles.

- Transmission gain is from 0 to 6 dB at frequencies from 300 to 1000 Hz, grazing angles below 6 degrees, all sea conditions with rms slopes greater than 3 degrees.

- Transmission gain is from 0 to -6 dB at frequencies from 300 to 1000 Hz, grazing angles greater than 6 degrees, all sea conditions with rms slopes greater than 3 degrees, and with source altitudes less than 500 ft.

- Sources at 500 ft have gains only above 800 Hz and below 30 degrees; below 800 Hz, losses of 1 to 2 dB occur at grazing angles above 30 degrees.

- Transmission gain tends to zero at locations approaching directly beneath the source.

The general trends of their experimental results may be explained by viewing the sea surface as a tilting plane with a non-zero most probable slope. Sound in air is refracted into the water through a locally flat interface whose size is on the order of the Fresnel zone $D = sqrt(2\,h\,\lambda)$, where h is the altitude of the source and λ is the wavelength of sound in air. The slope of the plane must satisfy Snell's law with respect to source and receiver positions. Thus, only the long wavelength portion of the surface wave spectrum will contribute.

Barger and Sachs also present an analysis of the expected number of specular refraction paths. That number is found to increase from near unity at low frequency and source height to about two at the highest frequency and wave height, which accounts for the increase of transmission gain for greater source altitude.

A.10 Coupling to long range propagation paths

"The normal-mode theory of air-to-water sound transmission in the ocean," D.M.F. Chapman and P.D. Ward, J. Acoust. Soc. Am. 87, 601-618 (1990).

This paper provides an excellent review and bibliography of earlier work and of the fundamentals of normal mode theory. The paper includes a rederivation of the basics for a point sound source in water and in air above the water. Their conclusions are consistent with an intuitive understanding of the problem:

- Normal mode functions and wavenumbers in the water do not change when the source moves from water into air; only the excitation of the modes by the source changes.

- The normal-mode excitation coefficients for both waterborne and airborne sources contain the same effective radiation patterns prescribed by ray theory.

- For the case of an airborne source the normal mode excitation coefficients are smaller for low-order modes than for high-order modes, corresponding to weak ray transmission in near horizontal directions, which is fully consistent with a ray interpretation.

Especially of interest are several computed results for transmission loss in water from a source in air at a height of 1000 m. The water is assumed to be isovelocity, 75 m deep, and overlying a variety of reflecting seabeds with varying amounts of acoustic loss. The results show signals extending to several kilometers in the water.

"Modeling air-to-water sound transmission using standard numerical codes of underwater acoustics," D.M.F. Chapman, D.J. Thomson and D.D. Ellis, J. Acoust. Soc. Am. 91, 1904-1910 (1992).

This paper discusses how to make use of standard underwater acoustic propagation models to address the signal in water from a source in air. Their primary conclusion is that for a distant receiver in water, transmission loss may be computed for a source of same strength close to the surface in water, and then reducing the pressure level (in dB) by the amount $20* \log(2\pi fd/c_a)$, where c_a is the sound speed in air.

A.11 Absorption of sound in air

"Atmospheric Absorption of Sound: Theoretical Predictions," L.B. Evans, H.E. Bass and L.C. Sutherland, J. Acoust. Soc. Am. 51, 1565-1575 (1972)

"Atmospheric Absorption of Sound: Analytic Expressions," H.E. Bass, H.-J. Bauer and L.B. Evans, J. Acoust. Soc. Am. 52, 821- 825 (1972)

The first of these two articles examines sound absorption in air as the result of several mechanisms. The air is considered as a mixture of four gases -- nitrogen, oxygen, carbon dioxide and water vapor. Loss mechanisms considered consist of (1) 24 energy trtansfer mechanisms in which translational and vibrational energy is transferred during binary collisions; (2) classical absorption losses comprising mostly losses from viscosity and heat conduction; and (3) additional relaxation losses involving rotational modes of the molecules. Their results show, for atmospheric conditions of present interest, absorption is relatively insensitivity to humidity, the CO_2 contributions are relatively unimportant, and the dominant losses at low frequency are related to vibrational relaxation processes. The results are claimed to be valid at 20 degrees C and over a 5 degree spread around 20 degrees. The useful output of the paper is a set of computed curves.

The second article extends the results of the first paper by presenting a relatively easy to use analytic result for absorption of sound in air at 20 degrees C over the frequency range 12 Hz to 1 MHz, and over all values of humidity. The result of this further analysis is that the 24 rates used to describe the vibrational relaxation mechanisms identified in the first article were replaced by

only three relaxation times and strengths at each humidity. Their primary result is the following equation for absorption.

$$\alpha = 27.26 \left\{ \Sigma_1^4 \ (f \, T_i \, A_i)/(1 + f^2 \, T_i^2) \ + 1.525.\text{x}10^{-9} f \right\} \ (f/c)$$

where α is the absorption coefficient in dB/1000ft,
    f is the sound frequency in Hz,
    c is sound speed in 1000ft/sec,
    T_i for i =1 - 4 are modified relaxation times in sec, whose values are determined as a function of humidity in the article
    A_i for i =1 - 4 are dimensionless relaxation strengths, whose values are determined as a function of humidity in the article.
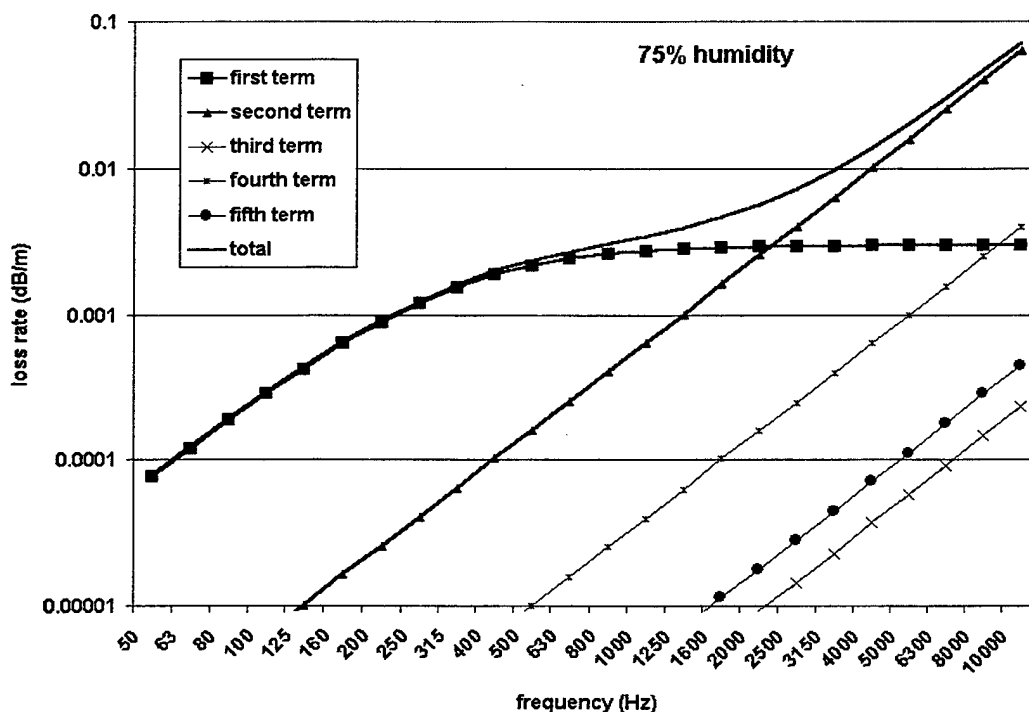

Figure A4. Separate contributions and total atmospheric absorption at
75% humidity, expressed in dB of loss over 1 wavelength, as a function of frequency.

The four relaxation terms and the linear-in-frequency term were computed and are plotted separately in Figure A4, along with the total absorption, giving the loss in dB/m. As a practical matter, the total absorption is well represented by only the first two terms.
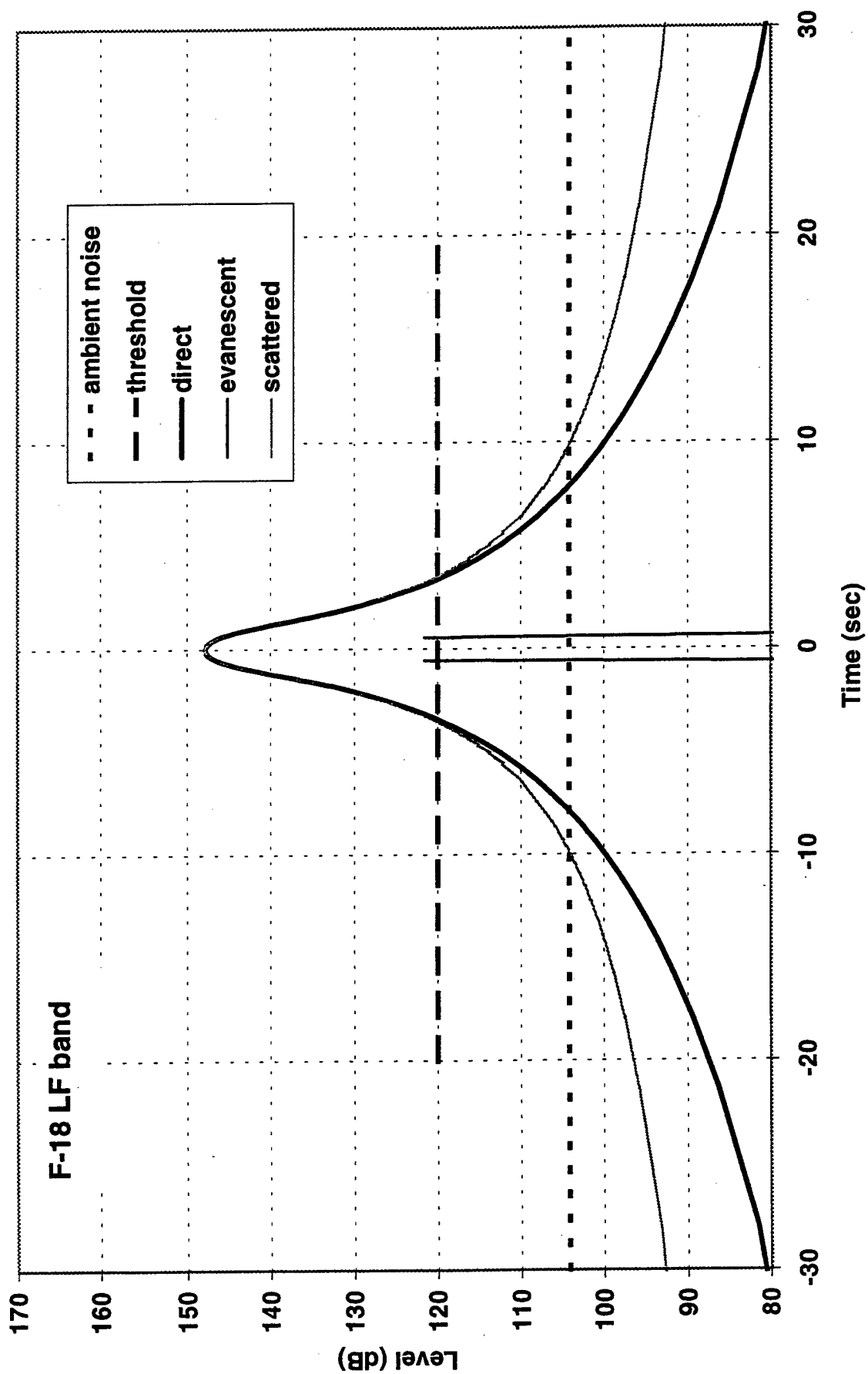
APPENDIX B. FLYOVER TIME SIGNATURES

Appendix B contains a collection of graphical displays of SPL vs time for aircraft flyovers. All figures are for the F-18 aircraft at 250 knots. The following 21 cases are presented:

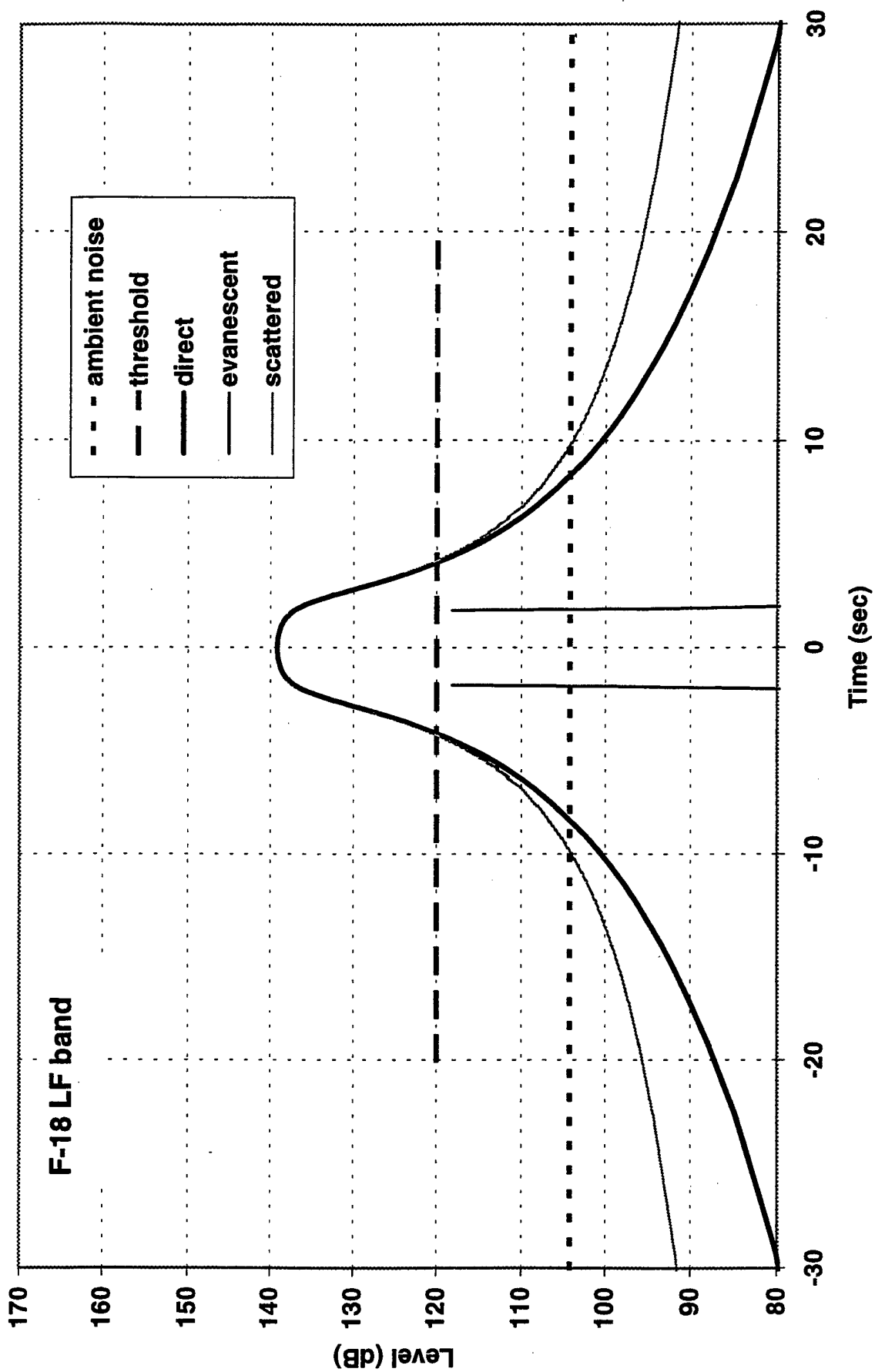| FIGURE	WATER DEPTH	RECEIVER (ANIMAL) DEPTH (m)	AIRCRAFT ALTITUDE ('HEIGHT') (m)	FREQUENCY BAND
1	Deep	50	300	LF
2	Deep	50	1000	LF
3	Deep	50	3000	LF
4	Deep	10	300	LF
5	Deep	10	1000	LF
6	Deep	10	3000	LF
7	Deep	2	300	LF
8	Deep	2	1000	LF
9	Deep	2	3000	LF
10	Deep	50	300	HF
11	Deep	50	1000	HF
12	Deep	50	3000	HF
13	Deep	10	300	HF
14	Deep	10	1000	HF
15	Deep	10	3000	HF
16	Deep	2	300	HF
17	Deep	2	1000	HF
18	Deep	2	3000	HF
19	Shallow	50	300	LF
20	Shallow	50	1000	LF
21	Shallow	50	3000	LF

In the figures the SPL is given in decibels referred to 1 μPa. Note also that peak estimates of ducted contributions for the shallow water cases are not realistically achievable, and the ducted estimates should be used only for time periods away from zero.
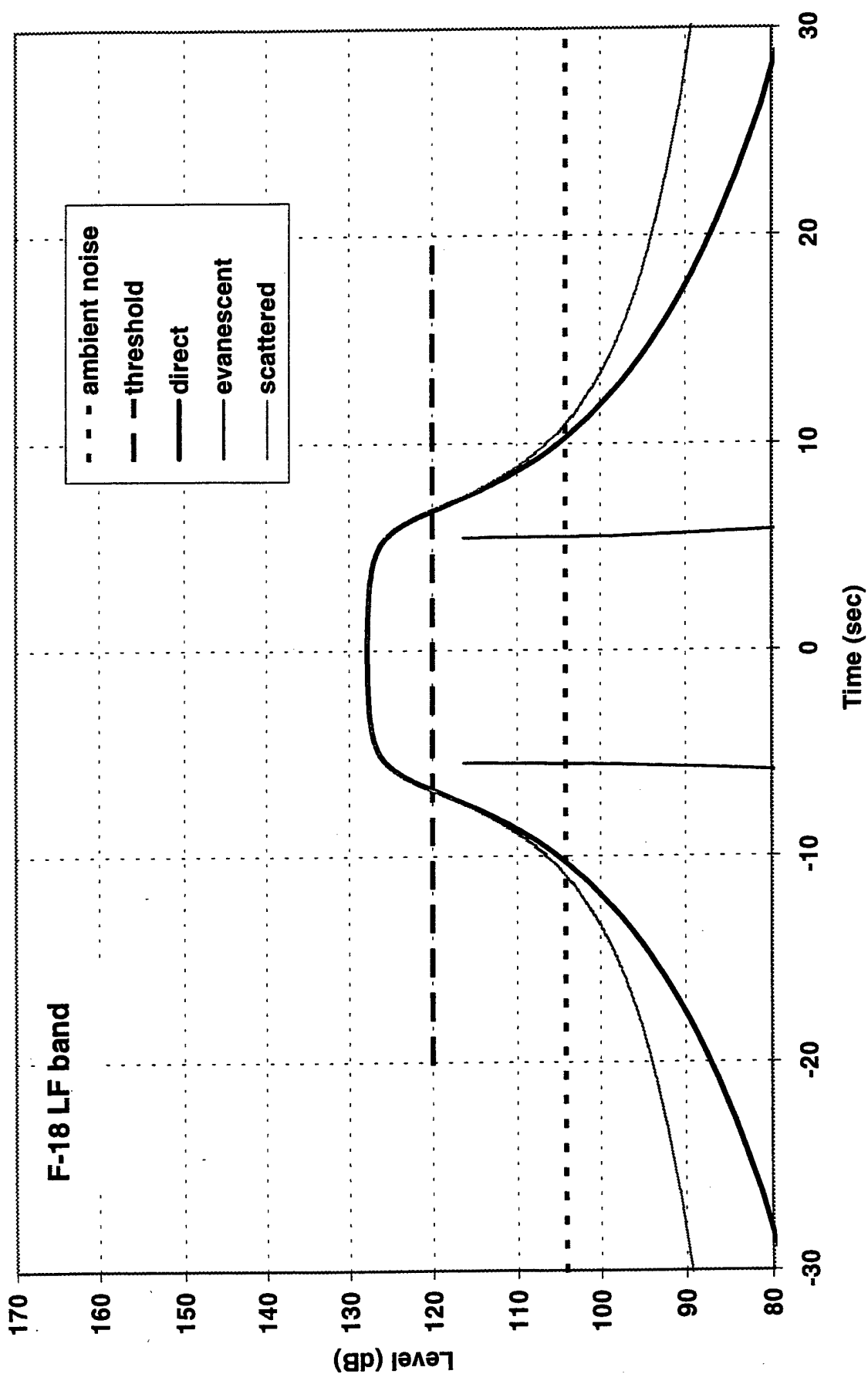
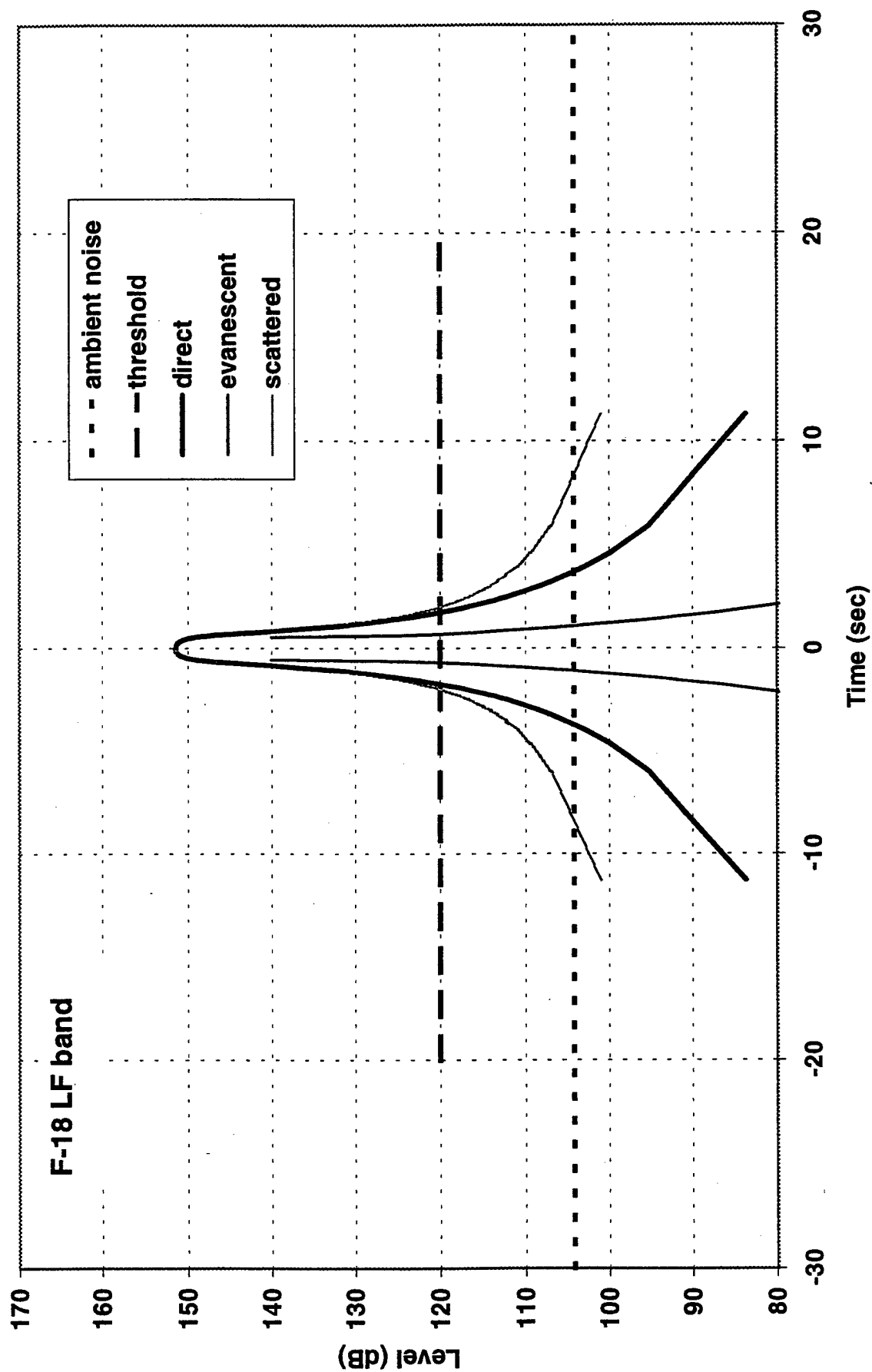time signature, overhead flyover, deep water   depth = 50 m height = 300 m

F-18 LF band

Legend:
- - - ambient noise
— threshold
—— direct
— evanescent
— scattered

Level (dB): 170, 160, 150, 140, 130, 120, 110, 100, 90, 80

Time (sec): -30, -20, -10, 0, 10, 20, 30

time signature, overhead flyover, deep water   depth = 50 m height = 1000 m

F-18 LF band

Legend:
- - - ambient noise
— threshold
— direct
— evanescent
— scattered

Level (dB)
Time (sec)

58

time signature, overhead flyover, deep water   depth = 50 m height = 3000 m

F-18 LF band

Legend:
- - - ambient noise
— threshold
— direct
— evanescent
— scattered

Time (sec)

Level (dB)

59

time signature, overhead flyover, deep water   depth = 10 m height = 300 m

F-18 LF band

Legend:
- - - ambient noise
— threshold
direct
evanescent
scattered

Level (dB): 170, 160, 150, 140, 130, 120, 110, 100, 90, 80

Time (sec): -30, -20, -10, 0, 10, 20, 30

time signature, overhead flyover, deep water   depth = 10 m height = 1000 m

F-18 LF band

Legend:
- - - ambient noise
— —threshold
—— direct
—— evanescent
—— scattered

Level (dB)

Time (sec)

61

time signature, overhead flyover, deep water   depth = 10 m height = 3000 m

F-18 LF band

Legend:
- - ambient noise
— threshold
—— direct
—— evanescent
—— scattered

Level (dB)
170
160
150
140
130
120
110
100
90
80

Time (sec)
-30   -20   -10   0   10   20   30

62

time signature, overhead flyover, deep water   depth = 2 m height = 300 m

F-18 LF band

Legend:
- ambient noise
- threshold
- direct
- evanescent
- scattered

Y-axis: Level (dB) — 80, 90, 100, 110, 120, 130, 140, 150, 160, 170

X-axis: Time (sec) — -30, -20, -10, 0, 10, 20, 30

63

time signature, overhead flyover, deep water   depth = 2 m height = 1000 m

F-18 LF band

Legend:
- ambient noise
- threshold
- direct
- evanescent
- scattered

Level (dB) — vertical axis: 80, 90, 100, 110, 120, 130, 140, 150, 160, 170

Time (sec) — horizontal axis: -30, -20, -10, 0, 10, 20, 30

time signature, overhead flyover, deep water   depth = 2 m height = 3000 m

F-18 LF band

Legend:
- ambient noise
- threshold
- direct
- evanescent
- scattered

Time (sec)

Level (dB)

time signature, overhead flyover, deep water   depth = 50 m height = 300 m

F-18 HF band

Legend:
- - - ambient noise
— threshold
— direct
— evanescent
— scattered

Time (sec)

Level (dB)

time signature, overhead flyover, deep water   depth = 50 m height = 1000 m

F-18 HF band

Legend:
- - - ambient noise
— threshold
direct
evanescent
scattered

Level (dB)

Time (sec)

time signature, overhead flyover, deep water   depth = 50 m height = 3000 m

F-18 HF band

Legend:
- - - ambient noise
— threshold
— direct
— evanescent
— scattered

Level (dB)

Time (sec)

68

time signature, overhead flyover, deep water   depth = 10 m height = 300 m

F-18 HF band

Legend:
- - - ambient noise
— — threshold
——— direct
——— evanescent
——— scattered

Time (sec)

Level (dB)

time signature, overhead flyover, deep water   depth = 10 m height = 1000 m

F-18 HF band

Legend:
- - - ambient noise
— — threshold
—— direct
—— evanescent
—— scattered

X-axis: Time (sec)
Y-axis: Level (dB)

time signature, overhead flyover, deep water   depth = 10 m height = 3000 m

F-18 HF band

Legend:
- - - ambient noise
— threshold
——— direct
——— evanescent
——— scattered

Time (sec)

Level (dB)

71

time signature, overhead flyover, deep water   depth = 2 m height = 300 m

F-18 HF band

Legend:
- - ambient noise
— threshold
— direct
— evanescent
— scattered

Level (dB)

Time (sec)

72

time signature, overhead flyover, deep water   depth = 2 m height = 1000 m

F-18 HF band

Legend:
- - - ambient noise
— — threshold
—— direct
—— evanescent
—— scattered

Level (dB) vs Time (sec)

time signature, overhead flyover, deep water   depth = 2 m height = 3000 m

F-18 HF band

Legend:
- - ambient noise
— — threshold
—— direct
—— evanescent
—— scattered

Level (dB)

Time (sec)

74

time signature, overhead flyover, shallow water   depth = 50 m   height = 300 m

F-18 LF band

Legend:
- - - ambient noise
— — threshold
—— direct
——— evanescent
——— scattered
—+— ducted

Level (dB)

Time (sec)

75

time signature, overhead flyover, shallow water   depth = 50 m height = 1000 m

F-18 LF band

Legend:
- ambient noise
- threshold
- direct
- evanescent
- scattered
- ducted

Time (sec)

Level (dB)

time signature, overhead flyover, shallow water depth = 50 m height = 3000 m

F-18 LF band

Legend:
- - - ambient noise
—— threshold
—— direct
—— evanescent
—— scattered
—+— ducted

Level (dB)

Time (sec)

77